

**A COMPARATIVE SERIAL ANALYSIS OF CARDIAC SARCOPLASMIC  
RETICULUM FUNCTION IN RATS SUBJECTED TO PRESSURE OR VOLUME  
OVERLOAD**

**BY**

**DANIJEL JURIC**

A thesis submitted to the

University of Manitoba

In partial fulfillment of the requirements for the degree of

**MASTER OF SCIENCE**

Department of Physiology & Faculty of Medicine

Institute of Cardiovascular Sciences

St. Boniface General Hospital Research Centre

Winnipeg, Manitoba

© **Danijel Juric, June 2007**

**THE UNIVERSITY OF MANITOBA**

**FACULTY OF GRADUATE STUDIES**

**\*\*\*\*\***

**COPYRIGHT PERMISSION**

**A COMPARATIVE SERIAL ANALYSIS OF CARDIAC SARCOPLASMIC  
RETICULUM FUNCTION IN RATS SUBJECTED TO PRESSURE OR VOLUME  
OVERLOAD**

**BY**

**DANIJEL JURIC**

**A Thesis/Practicum submitted to the Faculty of Graduate Studies of The University of  
Manitoba in partial fulfillment of the requirement of the degree**

**MASTER OF SCIENCE**

**DANIJEL JURIC © 2007**

**Permission has been granted to the University of Manitoba Libraries to lend a copy of this thesis/practicum, to Library and Archives Canada (LAC) to lend a copy of this thesis/practicum, and to LAC's agent (UMI/ProQuest) to microfilm, sell copies and to publish an abstract of this thesis/practicum.**

**This reproduction or copy of this thesis has been made available by authority of the copyright owner solely for the purpose of private study and research, and may only be reproduced and copied as permitted by copyright laws or with express written authorization from the copyright owner.**

## ACKNOWLEDGEMENTS

I would like to give my special thanks to my supervisor, Dr. Thomas Netticadan, for giving me the opportunity to be a part of his lab. Dr. Netticadan's guidance, advice, and unbelievable mentorship were instrumental in taking me to the completion of this research project. I would like to thank Dr. Netticadan for all motivating words of support throughout my training. I believe that the lessons he taught me will be an important tool in my future endeavors, professional and personal. I would also like to thank my committee members, Dr. Peter Zahradka, Dr. Michael Eze, Dr. Nasrin Mesaeli and Dr. Ian Dixon for their invaluable suggestions at different stages of my Master's Thesis.

My Master's training involved a great deal of interaction with exceptional members of Dr. Netticadan's lab, Elliott Cantor, Zainisha Vasanji, Mellissa Moyan, Jason Greville, Brian Chaze, Roop Sandhu, James Na and Keri Trout all of whom helped me a lot with different aspects of my work. I am thankful to all of you for being great colleagues and even better friends. In particular, I would like to thank Peter Wojciechowski with whom I have worked side by side on many different projects over the past few years. Peter has been an extraordinary friend, the friend one rarely finds in their lifetime.

I would like to acknowledge the Department of Physiology administrative staff Mrs. Gail McIndles and Mrs. Judith Olfert, and the department chair, Dr. Janice Dodd for their support with scholarship applications and assistance with other paperwork.

I was very fortunate to learn and to be trained at world renowned Institute of Cardiovascular Sciences at St. Boniface Hospital Research Centre. The numerous

interactions I had with the members of the Institute have greatly broadened my knowledge of the cardiovascular field.

For me, my family is the most important pillar of support and it goes without saying that I will always be thankful to my parents who understood my needs and sacrificed a lot to help me reach my goals.

My special thanks go to my dear friend Rowan Sharkey whom I have gotten to know in the final stages of my Master's training. Rowan has been an incredible source of support and happiness during this time. Rowan, *hvala* (thank you) for all the good times.

I would also like to acknowledge Postgraduate Master's Scholarship from Natural Sciences and Engineering Research Council of Canada (NSERC) in support of this project. A research grant from Canadian Institutes of Health Research (CIHR), Heart and Stroke Foundation of Manitoba (HSFM) and Manitoba Health Research Council (MHRC) to my supervisor, Dr. Thomas Netticadan, is hereby gratefully acknowledged.

## TABLE OF CONTENTS

	Page
Acknowledgements.....	i
Table of Contents.....	1
Abstract.....	2
List of Tables.....	4
List of Figures.....	5
I. Introduction.....	6
II. Literature Review.....	9
2.1 Heart Failure – Definition, Causes and Prevalence.....	9
2.2 General Cellular Events in Diseased Heart.....	9
2.3 Cardiac Hypertrophy – Definition and Causes.....	14
2.4 Pressure Overload (PO) versus Volume Overload (VO) Induced Cardiac Hypertrophy.....	15
2.5 Molecular Mechanisms of Cardiac Hypertrophy.....	16
2.6 Pathological versus Physiological Cardiac Hypertrophy.....	20
2.7 Calcium Handling in Normal Heart.....	22
2.8 Calcium Handling in Cardiac Hypertrophy and Heart Failure.....	26
2.9 Treatment Strategies for Hypertrophied and Failing Heart.....	29
2.10 Experimental Models of Cardiac Hypertrophy.....	31
III. Statement of Hypothesis.....	34
IV. Materials and Methods.....	35
V. Results.....	41
VI. Discussion.....	55
VII. References.....	71

## ABSTRACT

Left ventricular hypertrophy (LVH) refers to the compensatory enlargement of the heart aimed at reducing the stress caused by pressure overload (PO) or volume overload (VO) and maintaining adequate blood supply to tissues and organs; however, sustained hypertrophy leads to heart failure. The mechanisms underlying the transition from hypertrophy to heart failure are poorly understood. The aim of this study was to examine the involvement of cardiac sarcoplasmic reticulum (SR) in the development of contractile dysfunction due to PO or VO. We hypothesized that hypertrophy due to PO or VO will induce cardiac contractile dysfunction that will be associated with changes in the function of the SR. We also hypothesized that the alterations in SR calcium ( $\text{Ca}^{2+}$ ) handling and its regulation due to PO will be distinct from those induced by VO.

PO and VO were induced surgically by performing abdominal aortic banding and aortocaval shunt procedures, respectively. Cardiac structure and function were assessed via echocardiography at 2, 4, 16, and 28 weeks following the surgeries. SR function and its regulation were also examined. Over the course of the study, PO rats exhibited progressive thickening of LV walls while VO rats demonstrated progressive dilatation of LV cavity. Rats subjected to PO exhibited signs of diastolic dysfunction from 4 weeks onwards while systolic dysfunction became evident only after 28 weeks. In contrast, in VO rats, only systolic function was impaired at 16 as well as at 28 weeks. SR  $\text{Ca}^{2+}$ -uptake was enhanced in PO as early as 4 weeks, but not in the VO group. SR  $\text{Ca}^{2+}$ -uptake was elevated at 16 weeks, which corresponded to higher levels of sarco/endoplasmic reticulum  $\text{Ca}^{2+}$ -ATPase (SERCA2a) (in both PO and VO) and increased phosphorylation of phospholamban (PLB) at Ser16 and Thr17 (only in PO). At 28 weeks, SR  $\text{Ca}^{2+}$ -uptake

normalized to control levels in PO hearts while it still remained elevated in VO. Ratio of PLB:SERCA2a was unchanged in both PO and VO at 28 weeks. The observed reduction of the  $\text{Ca}^{2+}$ -uptake at 28 weeks in PO could be due to the increased activities of the phosphatases. Interestingly, in VO, reduced kinase and increased phosphatase activities did not impair SR function. We conclude that the progression of hypertrophy due to PO and VO in rats is accompanied by differential alterations in cardiac structure and function, as well as in SR function and its regulation.

## LIST OF TABLES

Table	Page
1. General characteristics of rats subjected to pressure overload (PO).....	46
2. General characteristics of rats subjected to volume overload (VO).....	47
3. Echocardiographic parameters of cardiac function and structure in rats subjected to 2, 4, 16 and 28 weeks of pressure overload (PO).....	48
4. Echocardiographic parameters of cardiac function and structure in rats subjected to 2, 4, 16 and 28 weeks of volume overload (VO).....	49



## LIST OF FIGURES

Figure	Page
1. SR $\text{Ca}^{2+}$ -uptake in 2-week (panel A), 4-week (panel B), 16-week (panel C) and 28-week (panel D) pressure overload (PO) and volume overload (VO) rats.....	50
2. Western blot analysis of sarco/endoplasmic reticulum $\text{Ca}^{2+}$ -ATPase (SERCA2a) (panel A), phospholamban (PLB) (panel B), Ser16 phosphorylated phospholamban (Ser16-PLB) (panel C) and Thr17 phosphorylated phospholamban (Thr17-PLB) (panel D) in 16-week pressure overload (PO) and volume overload (VO) rats.....	51
3. Western blot analysis of sarco/endoplasmic reticulum $\text{Ca}^{2+}$ -ATPase (SERCA2a) (panel A), phospholamban (PLB) (panel B), Ser16 phosphorylated phospholamban (Ser16-PLB) (panel C) and Thr17 phosphorylated phospholamban (Thr17-PLB) (panel D) in 28-week pressure overload (PO) and volume overload (VO) rats.....	52
4. SR-associated cyclic AMP-dependent protein kinase (PKA) activity (panel A) and $\text{Ca}^{2+}$ /calmodulin-dependent protein kinase II (CaMKII) activity (panel B) in 28-week pressure overload (PO) and volume overload (VO) rats.....	53
5. SR-associated protein phosphatase (PP) activity in 28-week pressure overload (PO) and volume overload (VO) rats.....	54

## I. INTRODUCTION

*Heart failure* is a leading cause of mortality in most parts of the developed world (4,8) and it is simply defined as the inability of the heart to deliver adequate amounts of blood to tissues and organs. Heart failure is a progressive condition that is often preceded by cardiac hypertrophy – a compensatory enlargement of the heart resulting from hemodynamic stress. As a consequence of the hypertrophic response to pressure overload (PO) or volume overload (VO), the heart undergoes remodelling by a series of changes in its structure and function (16,37,56,58). *Cardiac hypertrophy*, in its early stages, is an adaptive mechanism that offsets the stress the heart is subjected to; however, sustained hypertrophy leads to heart failure. There are many diseases, such as hypertension, ischaemic heart disease, valvular heart disease, myocarditis, cardiomyopathy and diabetes that are associated with abnormal hemodynamic load (PO or VO) on the walls of the heart and/or lead to the activation of the sympathetic nervous system, the renin-angiotensin system (RAAS) and various other mediators (3,5,6,16,37). Cardiac hypertrophy induced by either PO or VO are distinct phenomena likely mediated through different mechanisms (16,37,55-60). While PO results in concentric hypertrophy wherein the ventricular wall thickness increases without simultaneous chamber enlargement, VO results in eccentric hypertrophy wherein the chamber volume increases without any change in the ventricular wall thickness (16,56).

Volume overload is characterized by an increase in diastolic stress which induces replication of sarcomeres in series resulting in increased myocyte length and increased left ventricular cavity size. This remodeling process, also known as eccentric remodeling, allows the ventricle to increase its total stroke volume to compensate for the excess

volume. Pressure overload induces concentric remodeling of the left ventricle. Concentric remodeling is characterized by the replication of sarcomeres in parallel resulting in increased myocyte diameter, thereby leading to the thickening of the LV walls and the normalization of wall stress (16,37,55-60).

Contractile dysfunction is the hallmark of heart failure. It is now well established that the *sarcoplasmic reticulum* (SR), an intracellular membranous network, plays a central role in modulating cardiac contractility through its ability to regulate intracellular calcium ( $\text{Ca}^{2+}$ ) levels which are essential for cardiac contraction and relaxation (54,103,109). Due to its critical role in the control of intracellular  $\text{Ca}^{2+}$  homeostasis, irregularities in cardiac systolic and diastolic function can be linked to alterations in SR function (152-154). SR  $\text{Ca}^{2+}$ -uptake was reported to be compromised in PO and VO hearts (161-163,249,250); however, the major challenge lies in discovering the mechanisms by which this occurs.

The two major channel proteins associated with  $\text{Ca}^{2+}$ -release from the SR and  $\text{Ca}^{2+}$ -uptake back into the SR are the Ryanodine Receptor (RyR) and the sarco/endoplasmic reticulum  $\text{Ca}^{2+}$ -ATPase (SERCA2a), respectively (54,104,105,109,110,113). There are other important regulatory proteins, such as SR-associated c-AMP dependent protein kinase A (PKA),  $\text{Ca}^{2+}$ -calmodulin dependent protein kinase II (CaMKII), protein phosphatases I and II (PPI, PPII), phospholamban (PLB) and FKBP12.6, which can alter the activities of SR-associated channel proteins and thereby affect SR  $\text{Ca}^{2+}$  movement during contractile cycle of the muscle (106,117,118,122,192,255). It is therefore feasible that impairment of SR  $\text{Ca}^{2+}$ -cycling and regulatory proteins may lead to cardiac contractile dysfunction in the diseased heart.

The mechanisms underlying the transition from compensatory hypertrophy to heart failure still remain unclear and are therefore a prime area of cardiovascular research. The present study aims to examine the changes in cardiac contractile function and SR function and its regulation in well-established rat models of PO- and VO-induced hypertrophy leading to heart failure (199).

## **II. LITERATURE REVIEW**

### **2.1 Heart Failure – Definition, Causes and Prevalence**

Old and outdated definitions describe heart failure as a multifactorial syndrome wherein the heart's ability to pump sufficient blood to meet the metabolic demands of organs and tissues is compromised. The modern definition of heart failure, in addition to encompassing pathophysiology of the organ itself, also recognizes the importance of complex pathological alterations occurring at the cellular, subcellular, and molecular levels (1). Diseases such as hypertension, ischemic heart disease, valvular heart disease, cardiomyopathy, myocarditis, diabetes and others can often result in heart failure if left untreated (2-7).

Heart failure is a leading cause of mortality and it is a major public health problem in most parts of the world (4,8). In western societies, the incidence of death related to cardiovascular disease has approached the 50% mark and continues to rise dramatically (4,8-10). Such staggering numbers underscore the necessity of exploring new strategies in the treatment and prevention of heart failure and other cardiovascular conditions that might lead to heart failure. Research on the molecular mechanisms that underlie the progression of heart disease into heart failure will be an essential tool in devising new therapeutic interventions for combating this condition in the future.

### **2.2 General Cellular Events in Diseased Heart:**

Oxidative stress, necrosis, apoptosis, and fibrosis are pathophysiological events that are commonly observed/associated with the end-stage heart failure (overt heart failure) and cardiac hypertrophy (pre-heart failure stage) (4,11-16).

### **2.2.1 Oxidative Stress**

The progression of hypertrophy and the development of heart failure have been linked to oxidative stress (17-19). Reactive oxygen species (ROS), such as nitric oxide (NO), hydroxyl radical (OH·), superoxide anion (O<sub>2</sub><sup>-</sup>), hydrogen peroxide (H<sub>2</sub>O<sub>2</sub>) and peroxynitrite (ONOO<sup>-</sup>) are by-products of aerobic lifestyle (20). While at the same time playing a number of important regulatory and signaling roles, ROS have also been implicated in a number of pathophysiological conditions such as inflammation, cardiovascular diseases and neurodegenerative diseases (20-22). When present in abnormal quantities ROS can outcompete natural antioxidant defense systems, thus creating an imbalance (oxidative stress) which results in different pathologies. There is a strong association between heart disease and overactivation of the renin-angiotensin-aldosterone system (RAAS). It has been shown that increased levels of aldosterone and angiotensin II (Ang II) promote myocardial production of ROS which in turn cause cardiac dysfunction (23, 24). Several molecular studies have shown the overproduction of ROS is related to overactivation of NAD(P)H oxidase and xanthine oxidase, low levels of NO derived from endothelial nitric oxide synthase (eNOS) and a dysfunctional mitochondrial electron transport chain in hypertrophy and heart failure (4,23-27). Oxidative damages to mitochondrial electron transport chain proteins and mitochondrial DNA renders cells incapable of producing ATP, ultimately leading to an energy deficit, abruption of energy-demanding cellular processes and cell death (27-29). Another common feature of hypertrophy and heart failure is a lack of adequate perfusion of the organ in the face of increased oxygen demand (30). This also results in a depletion of energy stores (ATP and creatine phosphate) due to the lack of oxygen, thus reducing the

capacity of the cardiomyocytes to carry out oxygen-dependent, energy-yielding metabolic processes such as oxidative phosphorylation (1,28,31). Moreover, there are important antioxidant enzymes, such as superoxide dismutase (SOD) and glutathione peroxidase (GPx), the levels of which have been shown to be altered in hypertrophy and heart failure. The levels of these enzymes have been reported to be upregulated in a pressure overload (PO) model of cardiac hypertrophy and downregulated in heart failure (17,18).

### **2.2.2 Apoptosis**

Apoptosis is defined as “cell suicide” or “programmed cell death”. In contrast to necrosis, which is characterized by cell lysis and spillage of the intracellular material, apoptosis is characterized by the shrinkage, disintegration and removal of the cell in a “clean” fashion (32). Although the rate of apoptotic cell death was shown to be significantly elevated in ischemic heart disease, hypertrophy, and heart failure, the actual contribution and significance of apoptosis in progression of heart disease and in the development of heart failure has not been agreed upon yet (4). The apoptotic cascade can either be initiated at the level of cell surface receptors in which case it is termed the extrinsic apoptotic pathway or at the level of mitochondria in which case it is termed the intrinsic pathway (32,33). The activation of death receptors such as Fas/FasL or tumor necrosis factor receptor (TNFR) activates caspase 8 which in turn activates procaspase 3 (32,33). The activated and cleaved form of procaspase 3, caspase 3, then triggers the downstream proapoptotic machinery (32,33). Activation of the mitochondrial death pathway is triggered by intrinsic factors, such as oxidative stress and ischemia. Cellular stress can lead to the activation of proapoptotic Bax and Bad family proteins, which in turn leads to the release of cytochrome c (cyt c) from mitochondria by increasing the

permeability of the mitochondrial membrane (32,33). The release of cyt c ultimately results in the activation of caspase 3 which sets in motion the rest of apoptotic cascade (32,33). In addition to the stimulation of sarcolemmal receptors, apoptosis can also be initiated by hypoxia, oxidative stress, calcium overload, and by hormonal factors, such as Ang II and tumor necrosis factor-alpha (TNF $\alpha$ ) (13). Several groups have reported beneficial effects of apoptosis inhibition (via the inhibition of caspase signaling) on the heart in different experimental models (34-36). It has also been shown that apoptotic signaling inhibition results in the preservation of cardiac function as well as in the attenuation of maladaptive remodelling (36).

### **2.2.3 Fibrosis and ECM remodeling**

Fibrosis is defined as an excessive deposition of extracellular matrix (ECM) proteins, such as collagen and fibronectin (13). This matrix remodeling is commonly observed in the hypertrophied myocardium and is the result of an imbalance between deposition and breakdown of the matrix material. In the hypertrophied heart, the fibrotic process is usually a consequence of the stimulation of fibroblast proliferation by transforming growth factor-beta (TGF $\beta$ ) and other humoral factors, and is paralleled by an overproduction of collagen (13,16). Due to the overabundance of fibrillar collagens, overt fibrosis is associated with increased passive stiffness of the myocardium which leads to impaired relaxation as well as systolic dysfunction (13). The important regulators of interstitial matrix remodeling are matrix metalloproteinase (MMP) enzymes and their negative regulators, tissue inhibitors of MMPs (TIMPs). While MMPs are involved in the breakdown of fibrous material, TIMPs prevent further degradation by inhibiting the MMPs. Under normal conditions, the balance between MMP and TIMP activities is



tightly regulated, however, in the failing heart or in post-myocardial infarction (MI) remodelling there is an overactivation of MMPs thus leading to degradation of the ECM and subsequent cardiac dilatation (16,37,38).

#### **2.2.4 Neurohormonal Stimuli in Diseased Hearts**

It is well known that the adrenergic system and the RAAS are overactivated in the instances of hypertrophy and heart failure (13). It is also well established that  $\beta$ -adrenergic system gets activated when more load is placed on the heart, such as during the “fight or flight” response. Activation of the  $\beta$ -adrenergic system initiates a signaling cascade within the heart that improves contractility and increases heart rate, both of which is being required to meet the increased metabolic demands of the body. However, animal and human studies have demonstrated a reduced contractile response of the hypertrophied and failing heart to  $\beta$ -adrenergic stimulation (39-41). It seems that the overactivation, which is initially beneficial to the stressed myocardium, becomes maladaptive and inefficient if prolonged, and leads to increased energy demand, ischaemia, apoptosis and calcium imbalances (13). In heart failure patients, the heart is unable to perform well under situations of high physical stress due to the defective response of the heart to  $\beta$ -adrenergic stimulation. Overactivation of the adrenergic system leads to stimulation of MMPs which further exacerbate the pathological remodeling process (16,42) Activation of the RAAS and corresponding cellular signaling has been similarly associated with adverse cardiac remodeling, cardiac dysfunction, ROS overproduction, apoptosis and inflammation (4). Many studies have shown an increase in the levels of profibrotic cytokines (TGF $\beta$ ) and proinflammatory cytokines (TNF $\alpha$  and interleukin-6) in the failing hearts in response to RAAS activation (16,43,44). However,

stretch induced release of TNF $\alpha$  initially has salutary consequences as it has been shown that TNF $\alpha$  can interact with cardiotrophin 1 (CT-1) leading to gp130 receptor stimulation and subsequent adaptation in the instances of volume overload (VO) or antiapoptotic response in PO myocardium (16,45,46). On the other hand, prolongation of RAAS overactivation leads to oversecretion of TNF $\alpha$  and a negative outcome.

### **2.3 Cardiac Hypertrophy – Definition and Causes**

Heart failure is often preceded by cardiac hypertrophy although there are conditions that can result in heart failure, such as sudden cardiac death, without the involvement of the hypertrophic response. Cardiac hypertrophy refers to enlargement of the heart which is characterized by the increase in cardiac cell mass without concomitant cell proliferation. Many disease conditions that ultimately lead to heart failure are known to impose biomechanical stress on the heart resulting in cardiac remodeling and hypertrophy (10,13,47-49). Irrespective of the primary cause, the hypertrophic response is thought to be a compensatory mechanism in its initial stages as it allows the heart to counter the insult, and enable it to adapt and match the demands of the body. A compensatory hypertrophic response includes activation of the sympathetic nervous system, the RAAS and various other mediators (6,50-53). As a consequence of this response, the heart undergoes remodelling by a series of changes in its structure and function (6,37,50-55). Although hypertrophy may be beneficial to the stressed myocardium, sustained hypertrophy leads to heart failure. In the adult heart, the hypertrophic response is characterized by re-induction of fetal genotype, increased contractile protein synthesis, ECM remodeling, apoptosis, and restructuring of

myofibrils. These alterations ultimately lead to left ventricular (LV) heart failure (6,37,50-53,55).

## **2.4 Pressure Overload (PO) versus Volume Overload (VO) Induced Cardiac Hypertrophy**

Hypertrophy may be categorized into two types: pressure overload (PO) or volume overload (VO) (16,37,55-60). Cardiac hypertrophies induced by PO or VO are distinct phenomena likely mediated through different mechanisms (16,37,55-60). The mechanisms underlying the transition from hypertrophy to heart failure are poorly understood and are therefore a prime area of cardiovascular research.

### **2.4.1 Pressure Overload**

Pressure overload on the heart occurs in many clinical settings that include hypertension, mitral valve stenosis and aortic valve stenosis. When subject to one of these negative stimuli, the heart undergoes concentric remodeling in order to normalize wall stress from the increase in pressure placed on the cardiac tissue. Concentric remodeling of the LV involves thickening of the septal and posterior walls via the replication of sarcomeres (contractile units of a muscle) in parallel. Thus, an increase in pressure is reduced by an increase in wall thickness (16,37,55-60). In a clinical setting of hypertension, excess pressure is placed on the heart as it attempts to eject blood into the constricted and narrowed arteries (7). In aortic valve stenosis, the aortic valve cannot open properly thus placing additional pressure on the ventricles to pump blood through it (61). Hypertrophic cardiomyopathy is a genetic disease which is characterized by mutations of sarcomeric proteins that affect their contractile properties. These mutations

contribute to cardiac dysfunction, PO, and also concentric remodeling of the LV chamber (62).

#### **2.4.2 Volume Overload**

The other type of cardiac hypertrophy, VO, occurs in different clinical situations such as anemia, heart block, regurgitant mitral or aortic valves, atrial or ventricular septal defects, and other congenital diseases (16,37,55-60). The response to any one of these stimuli is eccentric hypertrophy and it results from an increase in diastolic stress which causes replication of sarcomeres in series, thereby increasing myocyte length and leading to increased chamber size (16,56). These changes allow the ventricle to increase its stroke volume to compensate for the excess volume of blood returning to the ventricle (16,37,55-60). In a clinical setting of mitral regurgitation, the mitral valve becomes defective and cannot close properly which in turn allows blood to flow back into the ventricles (63). In congenital heart disease, the presence of a hole in the septal wall (wall that divides left and right ventricle) enables abnormal blood flow between ventricles with an increased volume of blood entering the receiving ventricle (64). Increased venous return to the heart, and hence VO, also occurs in anemia when there is a reduction in the viscosity of blood and arterial dilatation (65).

#### **2.5 Molecular Mechanisms of Cardiac Hypertrophy**

The molecular mechanisms underlying the progression of cardiac hypertrophy from its developing stage to the decompensatory stage and ultimately heart failure have not been elucidated yet and thus remain an important focus of cardiovascular research. The cardiac hypertrophic response is initiated by a combination of mechanical and/or

hormonal factors resulting in the re-induction of certain genes which bring about the remodeling of cardiomyocytes (16,37,55-60,66,67).

### **2.5.1 Mechanotransduction in Cardiac Hypertrophy**

The exact mechanism detailing how an extracellular mechanical stimulus, such as PO or VO, is translated into biochemical signals inside the cell that ultimately results in the re-organization of contractile units (sarcomeres) is not well understood. There are currently two possible transducers, namely integrins and mechano-sensitive ion channels, which are thought to trigger the expression of certain hypertrophic genes by transmitting physical stress into a set of biochemical signals and molecular pathways inside the cell (67-70). Integrins transmit physical force by undergoing conformational changes which affect their binding interactions, or, indirectly, by passing on a mechanical stimulus to other adjacent cytoskeletal proteins (67). Mechano-sensitive ion channels adopt an open conformation in the presence of physical stress allowing an influx of  $\text{Ca}^{2+}$  ions. Once inside the cell,  $\text{Ca}^{2+}$  ions act as secondary messengers to activate calcineurin and calcium/calmodulin-dependent kinase II (CaMKII), among many other important calcium-dependent effectors (68). Once activated by  $\text{Ca}^{2+}$  ions, calcineurin and CaMKII become integrated into elaborate signal transduction pathways that ultimately alter gene expression. In addition to the aforementioned players, other candidates for mechanotransduction include the sarcomere, cytoskeletal elements such as microtubules, and the intranuclear stretch-induced changes in chromatin (67,70). Despite a relative lack of information on the topic, stretch-induced mechanotransduction is generally accepted to be an important component in the heart's ability to adapt to pathologic stimuli.

### 2.5.2 Hormonal Factors in Cardiac Hypertrophy

Cardiac hypertrophy can also be initiated by hormonal mediators. As with mechanotransduction, hormonal activation is also beneficial to the stressed heart; however, it contributes to maladaptive response down the line (16,37,55-60,67-70). Activation of the  $\beta$ -adrenergic system, and increased production of Ang II, endothelin (ET) and growth factors, either alone or in combination with other factors, stimulate cardiac remodeling. This stimulation is initiated at the level of G-protein coupled receptors (GPCRs) followed by the activation of Gs protein in the case of  $\beta$ -adrenergic system, or Gq protein in response to Ang II, ET, and growth factors. Upon  $\beta$ -adrenergic stimulation, Gs $\alpha$  associates and activates adenylyl cyclase (AC) which catalyzes the conversion of adenosine monophosphate (AMP) into cyclic AMP (cAMP) which in turn activates cAMP dependent protein kinase A (PKA) (71,72). PKA phosphorylates and regulates the function of  $\text{Ca}^{2+}$  handling proteins at the levels of the sarcolemma (the cell membrane of a muscle cell) and the sarcoplasmic reticulum (SR). Prolonged activation of PKA has been shown to lead to increased intracellular  $\text{Ca}^{2+}$  concentration (71,71). The outcome of  $\beta$ -adrenergic receptor activation is regulated downstream by the levels and the activity of stimulatory Gs proteins and inhibitory Gi proteins. The balance between Gs and Gi proteins determines the activity of AC. Hormones like Ang II lead to activation of Gq proteins which associate with different isoforms of phospholipase C-beta ( $\text{PLC}\beta$ ). PLC catalyzes the reaction in which phosphatidylinositol bisphosphate ( $\text{PIP}_2$ ) is converted into inositol 1,4,5-trisphosphate ( $\text{IP}_3$ ) and diacylglycerol (DAG), both important secondary messengers;  $\text{IP}_3$  leads to increases in intracellular  $\text{Ca}^{2+}$  and DAG activates protein kinase C (PKC) (71,72).

It has been shown that chronic activation of  $\beta$ -adrenergic receptor signaling can induce the development of pathological hypertrophy (53). Overexpression of the mediators of  $\beta$ -adrenergic signaling in the heart, namely,  $\beta(1)$ -adrenergic receptor (73), its associated G-protein,  $G\alpha$  (74), and its downstream effector, PKA, has been demonstrated to result in ventricular hypertrophy (75). However, a depression of  $G\alpha$  has also been linked to cardiac hypertrophy in PO and VO hearts (76). Similarly, it is well known that chronic activation of potent vasoconstrictor peptides such as Ang II, and ET-1 plays a prominent role in the pathogenesis of maladaptive hypertrophy (77-79). The prohypertrophic role of Ang II has been elucidated through studies wherein the cardiac overexpression of angiotensinogen (the precursor of Ang I), angiotensin converting enzyme (ACE) (which catalyzes the conversion of Ang I to Ang II) and Ang II receptor type I (AT1R) was shown to produce hypertrophy (77-79). The overexpression of ET-1 also resulted in ventricular hypertrophy (80). As with  $\beta$ -adrenergic signaling, the overexpression of ET-1 and Ang II signaling mediators, namely, Gq protein and its downstream effectors  $PKC\beta$  and  $PKC\epsilon$  has been demonstrated to result in cardiac hypertrophy (81,82). Pathological hypertrophic response has also been associated with cytokines, such as interleukin-1 (IL-1), IL-6 and TNF, and growth factors such as myotrophin, platelet-derived growth factor-C (PDGF-C),  $TGF\beta$  and nerve growth factor, the overexpression of which led to the development of cardiac hypertrophy (83-89).

Both hormonal factors and physical stress trigger a wide array of complex intracellular signaling pathways which result in altered gene expression and ventricular remodelling. Many of these pathways rely on important downstream effector molecules such as, calcineurin, CaMKII, PKA, glycogen synthase kinase 3 $\beta$  (GSK3 $\beta$ ) which have

been implied as mediators of maladaptive ventricular remodeling (16,37,55-60,90,91). These effectors, in turn, regulate the activity of several transcription factors via phosphorylation or dephosphorylation. The activation of transcription factors implicated in maladaptive remodeling, such as, inducible cAMP early repressor, nuclear factor of activated T cells (NFAT), myocyte enhancer factor 2 (MEF2) and GATA-4, re-induce the expression of different gene products (16,37,55-60,90,91).

## **2.6 Pathological Versus Physiological Hypertrophy**

### **2.6.1 Physiology of Pathological versus Physiological Remodelling**

As already stated, cardiac hypertrophy is defined as enlargement of the heart which is due to an increase in the size of the individual cardiomyocytes. The hypertrophic process is a part of a normal developmental process that enlarges the heart to match the increasing metabolic demands of the growing body (92). Developmental hypertrophy, therefore, is a physiological process which is beneficial and essential for survival. Cardiac hypertrophy also occurs as a result of pregnancy and physical exercise and it is commonly observed in trained athletes (4,93). The nature of physical exercise will also determine the kind of physiological remodeling and the final phenotype of the heart. For, example, isometric exercise, such as weight-lifting, imparts pressure overload on the heart resulting in concentric remodeling, whereas isotonic exercise, such as running or swimming, leads to eccentric remodeling which is due to volume overload (92,93,94). Pathological hypertrophy, as mentioned before, also develops as a result of PO and/or VO. However, while hemodynamic overload is intermittent in exercise-induced hypertrophy, the chronic stimulus that occurs in pathological hypertrophy might explain the maladaptive nature of hypertrophy in a clinical setting of PO and VO. In addition,



physiological hypertrophy is reversible upon termination of exercise regimen, whereas pathological hypertrophy in its advanced stages may only be partially reversed with treatment. However, due to the lack of efficient treatment strategies, cardiac hypertrophy as observed in different clinical settings is a major independent risk factor which predicts the subsequent development of heart failure.

### **2.6.2 Intracellular Signalling in Physiological versus Pathological Hypertrophy**

From a molecular point of view, pathological and physiological hypertrophy appear to be involved in recruiting different molecular pathways, although the exact mechanisms responsible for adaptive versus maladaptive cardiac remodeling have not been elucidated yet. It has been demonstrated that pathological hypertrophy is characterized by an increase of intracellular  $\text{Ca}^{2+}$  levels and the stress- or hormonally-induced activation of Gq/PLC/PKC pathway (95). In contrast, it has been shown by animal studies that exercise induced hypertrophy is associated with insulin-like growth factor I receptor (IGFIR) signaling which involves activation of the phosphatidylinositol 3-kinase (PI3K) and its downstream effectors, such as protein kinase B (Akt) (4,92,96-99). Inactivation of this pathway, by knocking out the *akt1* gene prevented exercise induced hypertrophy in rats (92,99). Inactivation of the same pathway in rats subjected to PO, however, did not prevent cardiac hypertrophy, which indicated this signaling molecule as one of the cellular markers capable of distinguishing pathological and physiological remodeling (57,95,96,98,99). Furthermore, it has been shown that overactivation of the p110 $\alpha$  isoform of PI3K has a protective role in a mouse model of PO and operates by attenuating pathological growth and fibrosis (100). On the other

hand, Ang II, TNF $\alpha$ , or ET-1 induced activation of p38, c-Jun N-terminal kinase (JNK) and PKC (some isoforms) has been implicated in pathophysiological signaling leading to maladaptive hypertrophy (4,92,95).

## **2.7 Calcium Handling in Normal Heart**

Calcium homeostasis is crucial for cardiac contraction and relaxation. Under normal physiological conditions, as the action potential gets propagated down the cell membrane, it ultimately reaches the t-tubules, which can be simply described as invaginations of the cell membrane. The t-tubule membrane contains dihydropyridine receptors (DHPR) or L-type voltage gated Ca<sup>2+</sup> channels in close proximity to the sarcoplasmic reticulum (SR). Depolarization of the t-tubules leads to the opening of L-type Ca<sup>2+</sup> channels on the sarcolemmal (SL) membrane of the t-tubules and subsequent entry of Ca<sup>2+</sup> from the extracellular space into the cell (54,101,102). This is termed inducer Ca<sup>2+</sup> as it binds to Ca<sup>2+</sup> release channels (RyR) on the SR causing these channels to open and release massive amounts of Ca<sup>2+</sup> from the SR into the cytosol (54,101,102). This process is thus termed Ca<sup>2+</sup>-induced Ca<sup>2+</sup> release (CICR) and is the major mechanism whereby the contraction of the heart is generated. The abundant release of Ca<sup>2+</sup> ions leads to contraction, which is mediated by the interaction of these ions with the contractile elements or myofibrils (54,101,102). Contraction is terminated when Ca<sup>2+</sup> dissociates from the myofibrils and is actively pumped back into the SR by sarco/endoplasmic reticulum Ca<sup>2+</sup> ATPase (SERCA), as well as by extrusion out of the cell by the sarcolemmal (SL) Sodium-Calcium Exchanger (NCX) and SL Ca<sup>2+</sup>-ATPase (54,101,102). SERCA accounts for the majority of Ca<sup>2+</sup> removal (75-90%, varies from species to species), whereas the SL Ca<sup>2+</sup> handling proteins account for the remainder

(54,103,104). Once the  $\text{Ca}^{2+}$  levels in the cytosol are reduced by the aforementioned processes, relaxation occurs and the cycle can take place again.

### **2.7.1 SR Function in Normal Heart**

It is now well established that the major player involved in regulating intracellular calcium ( $\text{Ca}^{2+}$ ) concentrations essential for cardiac contraction and relaxation is the sarcoplasmic reticulum (SR) (54). As mentioned earlier, SR  $\text{Ca}^{2+}$ -uptake occurs through SERCA2a (110 kDa), an integral protein present in the SR membrane. The function of SERCA2a is regulated by the low molecular weight protein phospholamban (27 kDa) which interacts with the cytosolic portion of SERCA2a (105-107). When in its unphosphorylated form, phospholamban (PLB) acts as a negative regulator of SERCA2a, thus preventing  $\text{Ca}^{2+}$ -uptake into the SR (106,107); yet upon phosphorylation by regulatory proteins such as CaMKII and PKA, this inhibition is relieved (107,108). Since SERCA2a accounts for the majority of  $\text{Ca}^{2+}$  re-sequestration into the SR and since the extent of SR loading determines the extent of subsequent  $\text{Ca}^{2+}$ -release, SERCA2a is therefore regarded as not only the major determinant of cardiac relaxation but also of cardiac contractility (109,110). Interestingly, it has been shown that a minor leak of  $\text{Ca}^{2+}$  from the SR of isolated cardiomyocytes through SERCA2a operating in reverse mode can generate ATP (111).

The release of  $\text{Ca}^{2+}$  from the SR occurs through the Ryanodine Receptor (RyR), an integral 565 kDa SR membrane protein (112,113). In cardiac muscle cells, RyR2 is the dominant isoform. The function of RyR2 is regulated by FK506 binding protein 12.6 (FKBP12.6) (112,113). Unlike PLB, FKBP12.6 does not inhibit RyR2 but rather stabilizes its closed conformation thus preventing diastolic leak of  $\text{Ca}^{2+}$  ions from the SR

and preserving optimal intraluminal SR  $\text{Ca}^{2+}$  levels (112,113). The RyR2 is also regulated by calsequestrin (CSQ), an intraluminal (45 kDa) SR protein concerned with  $\text{Ca}^{2+}$  storage. This interaction, however, is not direct and occurs through the formation of a complex that includes RyR2 and CSQ, as well as junctin and triadin, which are located in the SR lumen (114,115).

### **2.7.2 SR Regulation in Normal Heart**

The function of the SR is regulated through a balance between protein phosphorylation by kinases and dephosphorylation by phosphatases. In the heart, the activities and function of the SR-associated  $\text{Ca}^{2+}$  handling and regulatory proteins are modulated by kinases, such as CaMKII and PKA, and phosphatases, such as protein phosphatase I (PPI) and protein phosphatase 2A (PP2A) (116-119). Specific regulation of  $\text{Ca}^{2+}$  handling proteins is attained through anchoring proteins that allow the formation of complexes wherein the kinases and phosphatases are brought into close proximity of their target SR proteins (119,120). The localization of kinases and phosphatases relative to the SR membrane facilitates their interaction with SR membrane proteins, allowing them to specifically target and control the status of the SR proteins.

It has been reported that both PKA and CaMKII are endogenous to the SR having the ability to phosphorylate various SR proteins (121-123). It is well known that both PKA and CaMKII promote  $\text{Ca}^{2+}$ -uptake by phosphorylating PLB which in turn disinhibits SERCA2a and allows it to pump more  $\text{Ca}^{2+}$  into the SR (106,107). When it comes to phosphorylation of PLB, PKA mediates phosphorylation at Serine 16 (Ser16) residue while CaMKII targets the Threonine 17 (Thr17) residue. The phosphorylation of Ser16 is reported to be required for subsequent phosphorylation of Thr17 (124,125);

however, both are thought to improve  $\text{Ca}^{2+}$ -uptake by increasing  $V_{\text{max}}$  and/or increasing the affinity of SERCA2a for  $\text{Ca}^{2+}$  (124-129). Direct phosphorylation of SERCA2a by CaMKII at the Ser38 has also been reported and this modification has been shown to promote  $\text{Ca}^{2+}$ -uptake as well (130-132). However, this finding has been challenged by some other studies which showed no change in  $\text{Ca}^{2+}$ -uptake upon phosphorylation of SERCA2a by CaMKII (133,134).

The rate of  $\text{Ca}^{2+}$ -release is determined by the open probability of RyR channels. It has been reported that PKA-dependent phosphorylation of RyR2 at Ser2809 residue stimulates the open conformation of RyR2 and thus promotes  $\text{Ca}^{2+}$ -release (113,135-137). The phosphorylation of RyR2 is thought to increase dissociation of FKBP12.6 from the channel which, in turn, would favor its open state (113). This view, however, has been challenged as some studies have shown that PKA-mediated phosphorylation of RyR2 does not affect the rate of  $\text{Ca}^{2+}$ -release from the SR (138). In addition, CaMKII has also been shown to positively regulate  $\text{Ca}^{2+}$ -release through RyR2 by increasing the responsiveness of the channel to  $\text{Ca}^{2+}$  ions and increasing its open probability (139). As with PKA, CaMKII can phosphorylate at Ser2808/2809 as well as at Ser2815, which appears to be the CaMKII specific target site on RyR2 (139,140). There is less information available in the literature on the status of protein phosphatases in the context of SR regulation in the heart. The two major PPs present in the heart are PP1 and PP2A and they account for 90% of phosphatases in the heart (141,142); other important subtypes of the PP2 family include PP2B and PP2C (141,142). PP1 has been shown to negatively regulate  $\text{Ca}^{2+}$ -uptake by dephosphorylating PLB at both Ser16 (PKA site) and Thr17 (CaMKII site) thus leading to increased inhibition of SERCA2a (143,144). The

rate of  $\text{Ca}^{2+}$ -release may also be regulated through dephosphorylation of RyR2 by PP1, PP2A, and PP2B which could in turn reduce the extent of  $\text{Ca}^{2+}$ -release (113,119,145).

## **2.8 Calcium Handling in Cardiac Hypertrophy and Heart Failure**

Many studies have implicated aberrant  $\text{Ca}^{2+}$  handling in cardiac hypertrophy and other cardiovascular diseases. The intracellular  $\text{Ca}^{2+}$  concentration is predominantly regulated by the SR. Upon stimulation, this organelle releases  $\text{Ca}^{2+}$  into cytosol where it interacts with contractile proteins and induces a series of conformational changes in these proteins resulting in cardiac contraction. Relaxation occurs as the levels of  $\text{Ca}^{2+}$  return to normal via active  $\text{Ca}^{2+}$  re-uptake back into the lumen of the SR. Several studies have reported abnormal  $\text{Ca}^{2+}$  handling in PO at the level of the SL as well as the SR. The activity of sarcolemmal L-type  $\text{Ca}^{2+}$  channel was found to be unaltered in the compensated stage and increased in the decompensated stage of PO-induced hypertrophy (146,147). Other studies have reported reduced activity of NCX in compensatory hypertrophy, induced by aortic banding, in spite of increased expression of the exchanger (148). Oxidative stress, which is known to occur in hypertrophied and failing hearts, has been implicated in altered  $\text{Ca}^{2+}$  handling by the SL as well as the SR (22,149-151).

### **2.8.1 Sarcoplasmic Reticulum in Heart Disease**

Contractile impairment is the hallmark of heart failure. Due to its critical role in the control of intracellular  $\text{Ca}^{2+}$  homeostasis, irregularities in cardiac function have been linked to alterations in SR function (152-154). Numerous studies have reported changes in SR function as well as the status of SR-associated  $\text{Ca}^{2+}$  handling proteins in diseased heart (152-158). The importance of SERCA2a and RyR2 has been demonstrated in mouse knockout studies. Deletion of the SERCA2 gene generated no homozygous

mutants, whereas absence of the RyR2 gene resulted in embryonic lethality in mice (159,160). Therefore, these proteins are absolutely essential for life.

While earlier reports have suggested that SR  $\text{Ca}^{2+}$ -uptake was compromised in PO hearts (161,162) and VO hearts (163), the major challenge lies in discovering the mechanisms by which this occurs. So far it has been well established that SERCA2a and the phosphorylation status of PLB play a major role in determining the rate of  $\text{Ca}^{2+}$  re-uptake. Most studies have therefore concentrated on examining the involvement of these proteins in PO models. It has been demonstrated that PO results in the reduction of  $\text{Ca}^{2+}$ -uptake, protein levels and activity of SERCA2a, and mRNA levels of SERCA2a and PLB at different stages of hypertrophy (152-158,164,165). Others have shown inconsistent findings in spontaneously hypertensive rats (SHR) which is a genetic model of PO. These studies have shown varying results in terms of  $\text{Ca}^{2+}$ -uptake as well as SERCA2a activity, protein and mRNA levels (166-168). One study has shown no change in SERCA2a and PLB in the compensated stage of hypertrophy in SHR (169).

Although there is a general lack of information on the mechanisms behind cardiac dysfunction in PO-induced hypertrophy and heart failure, a few studies have shed some light on the importance of SR regulatory mechanisms in diseased hearts (170,171). An increase in CaMKII- $\delta$  content has been observed in the SHR model at the developing hypertrophy stage (172). In the same model, another group has reported enhanced PLB phosphorylation which reflected an increase in the activities of both PKA and CaMKII without concomitant alterations in protein phosphatases (166).

Cardiac dysfunction has also been attributed to impaired  $\text{Ca}^{2+}$ -release. The decrease in  $\text{Ca}^{2+}$ -release may be due to a depletion of SR  $\text{Ca}^{2+}$ . The decrease in SR  $\text{Ca}^{2+}$

load is thought to be brought about by an increase in extrusion via NCX (which is found to be upregulated in heart failure), RyR2 hyperphosphorylation (which results in diastolic leak of  $\text{Ca}^{2+}$  from the SR), and reduced SR  $\text{Ca}^{2+}$ -uptake (173-175). Release of  $\text{Ca}^{2+}$  from the SR has been shown to be reduced at different stages in the aortic banding model of hypertrophy along with a depression in the levels of both RyR2 protein and mRNA (178,179). On the other hand, one study has shown no change in RyR2 in the compensated stage of hypertrophy in the SHR (169).

Recent work has implicated defects occurring at the level of RyR2 as key in the deterioration of SR function. For instance, different studies have shown hyperphosphorylation of the RyR2 by both PKA and CaMKII to be associated with dissociation of FKBP12.6 from the RyR2 and subsequent spontaneous  $\text{Ca}^{2+}$  leak from the SR which, in turn, causes delayed afterdepolarizations, ventricular arrhythmias, maladaptive remodeling and cardiac contractile dysfunction (113,117,175-177). In addition, miscommunication between L-type  $\text{Ca}^{2+}$  channels and the RyR2 specifically decreased responsiveness of RyR2 to extracellular  $\text{Ca}^{2+}$  entry and has been shown to be associated with decreased  $\text{Ca}^{2+}$  transients and reduced contractility (180). The intermolecular defects between L-type  $\text{Ca}^{2+}$  channels and the RyR2 have been attributed to a decrease in the protein levels of junctophilin which anchors the SR membrane to the SL membrane (180). However, at present, there is a lack of a widely shared consensus regarding regulation of the RyR2 in hypertrophy and HF. This area, however, holds great promise, and combating heart failure via modulation of a leaky RyR2 is a likely focus of future work.



## 2.9 Treatment Strategies for Hypertrophied and Failing Heart

As already stated, cardiac hypertrophy is an important predictor for subsequent heart disease that can lead to heart failure. The progression of hypertrophy from the adaptive to the maladaptive stage and heart failure is poorly understood and is currently a prime area of cardiovascular research. In addition, cardiac hypertrophy is an established independent risk factor for subsequent development of heart failure. Therefore, a major emphasis is being placed on discovering molecules and pathways that promote the hypertrophic response, as well as on pathways that blunt or prevent the adverse remodeling process. In an attempt to prevent hypertrophy from progressing into heart disease, therapeutic approaches that target well-known hypertrophic pathways, such as  $\beta$ -adrenergic signaling pathway as well as the RAAS are being investigated. Although, the benefits of  $\beta$ -blockers, ACE inhibitors and Ang II receptor blockers have been linked to a reduction in the hypertrophic response, complete reversal of the condition has not been shown in patients receiving these agents (5-7). Recently, the antihypertrophic potential of treatment with statins (hydroxymethylglutaryl-coenzyme A reductase inhibitors) has been explored. Despite showing an ability to prevent the hypertrophic response, statins caused a depletion of low density lipoprotein (LDL) and coenzyme Q10, which limits their use in a clinical setting (181,182).

Studies have shown that overexpression of several endogenous proteins, such as GSK3, caveolin 3, phospholipase A2, peroxisome proliferator-activated receptor, histone deacetylase 9 and inositol polyphosphate 1-phosphatase prevented hypertrophy while their downregulation has been reported to promote hypertrophy (90,183). Therefore,

upregulating the levels of these molecules might provide another promising strategy for prevention and/or treatment of maladaptive cardiac hypertrophy.

### **2.9.1 Gene Therapy – SR Targets**

Many studies have linked cardiac dysfunction to abnormalities in the function and the regulation of the SR (152-154,170). Therefore, SR proteins continue to be attractive therapeutic targets for the treatment of cardiac disease. SERCA2a has been shown to be a major determinant of cardiac contractility and its activity is often found to be reduced in failing hearts. The activity of SERCA2a is determined by the level of SERCA2a protein as well as the level and phosphorylation status of its negative regulator PLB. Gene therapy approaches, aimed at restoring or increasing the levels of SERCA2a in failing rat hearts, have shown promising results. These studies, conducted using adenoviral transfer of SERCA2a into the failing hearts, showed an improvement in contractility (184,185). One study showed that despite improving cardiac contractile function in a large animal model of diastolic dysfunction, SERCA2a gene transfer resulted in a reduced cardiac response to  $\beta$ -adrenergic stimulation (185). Although a reduction of PLB has been viewed as a promising approach for enhancing SR  $\text{Ca}^{2+}$ -uptake by disinhibiting SERCA2a and improving cardiac function in failing hearts (187,188), one human study has reported that the deletion of PLB results in dilated cardiomyopathy (189). In addition, there also appears to be a link between mutations in PLB and the development of heart failure in humans (190). Dephosphorylation of PLB, which is mediated by PPs, is a major cause of depressed SERCA2a function in diseased hearts (170,191,192). Therefore, the inhibition of PPs could be another useful therapeutic approach for preserving SERCA2a function in hypertrophied and failing hearts. Along these lines, one study has recently

reported beneficial effects of overexpressing PP1 inhibitor (inhibitor 1) on cardiac remodeling and cardiac dysfunction in mice subjected to PO (193). Defective RyR2 gating has been recognized as a critical abnormality in arrhythmias and heart disease progression making this channel protein another attractive molecular therapeutic target in heart failure (113,117,194,195). Along those lines, the restoration of the function of hyperphosphorylated RyR2 has been reported via generation of FKBP mutant protein with a higher binding affinity for RyR2 (196). Diastolic leakage and cardiac dysfunction have also been prevented via treatment with the 1,4-benzothiazepine derivative, JTV519, which is a RyR2 stabilizing molecule that binds to the channel and increases FKBP affinity for RyR2 (194,197,198).

## **2.10 Experimental Models of Cardiac Hypertrophy**

### **2.10.1 Advantages of Animal Models**

Animal models of progressive cardiac hypertrophy and heart failure have been invaluable in studying comparable human conditions. The suitability of animal models is founded on the fact that human hearts at different stages of hypertrophy, namely developing, compensatory and decompensatory stage, are difficult to obtain. What this means is that human samples can only be obtained from end-stage heart failure patients when only maladaptive mechanisms can be studied. Therefore, the progressive nature of cardiac hypertrophy and the underlying molecular mechanisms can only be followed via experimental animal models. Moreover, in contrast to animal samples, human hearts are “impure” in the sense that they often have been exposed to various treatment interventions that target the heart as well as other ailments. Animal tissues, on the other hand, can be obtained in their controlled form where the only variable affecting organ

function is the causal physiological event, such as the case with pressure or volume overload. Our experimental rat models of PO and VO, induced surgically by well established aortic banding and aortocaval (AV) shunt procedures, respectively, are well suited to address the above concerns. Furthermore, since in our models, hypertrophy is induced by hemodynamic overload, this simulates what happens in the clinical setting. These models, therefore, provide a better alternative to studying the condition than genetic means wherein the alterations in gene expression could account for the remodeling process. Based on the studies done so far, the models that we employ are fairly reproducible and are ideal for studying the transition of hypertrophy from compensated to decompensated stage (199).

#### **2.10.2 Pressure Overload Models**

Abdominal aortic banding (AAB) has been used by many groups to simulate PO as seen under clinical situations, such as hypertension and valvular stenosis (200,201). The abdominal aortic banding procedure is performed by tying a ligature around the suprarenal aorta. Transverse aortic constriction (TAC), on the other hand, is performed at the level of the aortic arch and its proximity to the heart induces higher pressure on the organ compared to AAB (202). The one-kidney, one-clip (1K1C) procedure involves the removal of one kidney and the placement of a metal clip on the opposite renal artery thus producing a luminal stenosis which induces systemic hypertension (203,204). A model of pulmonary constriction is commonly used when studying right ventricular hypertrophy and is generated by banding the pulmonary artery or by injecting monocrotaline which induces pulmonary hypertension (157,205).

### **2.10.3 Volume Overload Models**

For almost two decades the aortocaval (AV) shunt has been widely used to mimic the clinical condition of VO which manifests under the conditions of mitral regurgitation and anemia (206,207). An aortocaval shunt is constructed between the renal arteries and iliac bifurcation by puncturing the aorta with a needle, which is inserted through to the vena cava (208,209). An AV shunt procedure can also be performed at the aortopulmonary level as well as between left common carotid artery and external jugular vein (210,211). Anemia can be induced by creating iron-deficiency, typically achieved by reducing dietary iron intake (in combination with bleeding) (212,213). Volume overload can also be induced by creating an atrio-ventricular (A-V) block by insertion of an electric knife through the right atrial wall followed by electrocoagulation of the nodal region (214). Mitral valve regurgitation is surgically created by advancing a catheter to the left atrium followed by grasping and disrupting mitral valve chordae tendinae (215,216). Similarly, tricuspid valve regurgitation and aortic valve regurgitation are created by cutting tricuspid valve chordae tendinae and rupturing the aortic leaflet, respectively (217,218).

### **2.10.4 Combination of Pressure and Volume Overload**

The contribution of both PO and VO in the development and progression of hypertrophy can also be studied using an experimental model of myocardial infarction (MI) created by coronary artery ligation. This model mimics the clinical situation of ischemic heart disease and is a mixture of PO and VO (16,219).

### III. STATEMENT OF HYPOTHESIS

We hypothesize that pressure overload (PO) and volume overload (VO) in the advanced stages will induce abnormalities in SR function ( $\text{Ca}^{2+}$ -uptake) and its regulation by protein phosphorylation and dephosphorylation. In addition, changes in SR protein composition will contribute to progression of hypertrophy from the compensated to the maladaptive stage with impaired cardiac function. We also hypothesize that PO will induce changes in SR function and its regulation which will be distinct from the alterations induced by VO.

The aims of this study will be accomplished by examining the effects of PO or VO on cardiac structure and performance, and SR function and its regulation at 2, 4, 16 and 28-weeks. Cardiac structure and performance will be analyzed via echocardiography. The specific parameters pertaining to SR function/regulation will include: SR  $\text{Ca}^{2+}$ -uptake; protein levels of SR  $\text{Ca}^{2+}$  cycling and regulatory proteins, SERCA2a and PLB, respectively, and PLB phosphorylation status (Ser16-PLB, Thr17-PLB); SR-associated kinase (CaMK and PKA) activities and SR-associated protein phosphatase (PP) activities. The results of this work will shed important light on the mechanisms underlying contractile dysfunction in PO- versus VO-induced hypertrophy in male Sprague-Dawley rats. The findings will aid in identifying mechanisms behind SR dysfunction and thus in unraveling possible therapeutic targets for improving cardiac function in these two distinct forms of cardiac hypertrophy.

#### IV. MATERIALS AND METHODS

The following experimental protocols were approved by the Animal Care Committee of the University of Manitoba and are in agreement with the *Canadian Council on Animal Care Concerning the Care and Use of Experimental Animals* (Vol. 1, 2<sup>nd</sup> Edition, 1993).

##### **Creation of the animal models**

Male Sprague-Dawley rats weighing 150-200 g were subjected to abdominal aortic banding (200) and aortocaval shunt (206) procedures as described previously by us and others (199,200,206). Briefly, 5-week-old rats were kept in a temperature and humidity-controlled room with a 12-hour light to 12-hour dark cycle for one week prior to creation of the PO and VO models. Standard rat chow and tap water were available *ad libitum*. PO was induced via the abdominal aortic banding method, while VO was induced via the aortocaval shunt method. All rats were anesthetized for surgery with 5% isoflurane carried by oxygen at a flow rate of 2 L/min. Rats were then maintained in surgical plane of anesthetic with 2% isoflurane. For PO, a midline laparotomy was performed and the suprarenal abdominal aorta was exposed. A silk suture was used to tie off the vessel using a blunt 21-gauge needle as a guide. Successful bands were snug while maintaining blood flow to the kidneys and lower extremities. For VO, a midline laparotomy was performed and the abdominal aorta and vena cava were exposed by blunt dissection between the renal arteries and the iliac bifurcation. An 18-gauge needle was inserted into the exposed aorta at a 45° angle and pushed through to the vena cava, creating the shunt. Cyanoacrylate (Krazy Glue, Elmer's Product Canada, Toronto, ON) was used to seal the puncture. In successful VO rats, oxygenated blood from the

abdominal aorta could be seen mixing in the vena cava. In both models, the abdominal musculature and the skin incisions were closed by standard techniques with absorbable suture and autoclips. Sham operated animals served as controls for both groups and were subjected to the same surgeries except for the creation of the band or the shunt. Rat housing conditions, as described above, remained constant throughout the duration of the 28-week experiment.

### **Echocardiography**

Two, four, sixteen and twenty-eight weeks post-surgery, rats were weighed and anesthetized using isoflurane as described previously. Transthoracic two-dimensionally (2D)-guided M-mode echocardiography and Pulse Wave Doppler echocardiography were performed using a Sonos 5500 ultrasound system (Agilent Technologies, Andover, MA) equipped with a 12 MHz (s12) transducer. For M-mode recordings, the parasternal short-axis view was used to visualize the left ventricle in 2-D at the level of the papillary muscles with a depth setting of 3 cm. M-mode recordings were then analyzed at a sweep speed of 150 mm/s with the axis of the probe aligned with the middle of the ventricle. The following parameters were measured using the leading edge method described by the American Society of Echocardiography (220): percentage of left ventricular fractional shortening (%FS), left ventricular ejection fraction (EF), cardiac output (CO), heart rate (HR), left ventricular internal dimensions at both diastole and systole (LVIDd and LVIDs, respectively), left ventricular posterior wall dimensions at diastole and systole (LVPWd and LVPWs, respectively) and interventricular septal dimensions diastole and systole (IVSd and IVSs, respectively).



The Doppler measurements were taken using the apical 5-chamber view to assess isovolumic relaxation time (IVRt), which is the time from aortic valve closure to the onset of mitral flow. Values obtained for statistical analysis were average data collected from three cardiac cycles.

### **General characteristics**

After the 2, 4, 16 and 28-week echocardiographic assessments, rats were weighed and anesthetized using a cocktail of ketamine (90 mg/kg) and xylazine (10 mg/kg) prior to sacrifice. Hearts were removed, washed in ice-cold saline and their weights were measured. Left ventricular tissue was separated, flash-frozen in liquid nitrogen and subsequently stored at  $-85^{\circ}\text{C}$  until used for further experimentation. Lungs and liver were removed, washed in ice-cold saline and wet weights were recorded. The organs were then set to dry, and subsequently to be weighed again.

### **Preparation of SR vesicles**

SR vesicles were obtained by a method described previously (221-225). Left ventricular tissue was pulverized and homogenized with a polytron homogenizer (Brinkmann, Westbury, NY) in a buffer containing: 10 mM  $\text{NaHCO}_3$ , 5 mM  $\text{NaN}_3$ , 15 mM Tris-HCl at pH 6.8 (10 ml/g tissue). The homogenate was centrifuged for 20 min at  $10,919 \times g$ . The resultant pellet was discarded and the supernatant was further centrifuged for 45 min at  $43,666 \times g$ . (Beckman, JA 20). The resultant pellet was resuspended in a buffer containing 0.6 M KCl and 20 mM Tris-HCl (pH 6.8) and centrifuged for 45 min at  $43,666 \times g$ . The final pellet containing the SR fraction was suspended in a buffer containing 250 mM sucrose and 10 mM histidine, pH 7.0. This was aliquoted and frozen in liquid nitrogen prior to storage at  $-85^{\circ}\text{C}$ . All buffers used for

isolation contained a cocktail of protease inhibitors consisting of 1  $\mu$ M leupeptin, 1  $\mu$ M pepstatin, and 100  $\mu$ M phenylmethylsulphonyl fluoride to prevent protein degradation during the isolation procedure. The protein content of the SR fraction was determined using the Lowry method (226).

#### **Measurement of SR $\text{Ca}^{2+}$ -uptake**

SR  $\text{Ca}^{2+}$ -uptake was measured by a procedure described earlier (221-225). The reaction mixture contained: 50 mM Tris-Maleate (pH 6.8), 5 mM  $\text{NaN}_3$ , 5 mM ATP, 5 mM  $\text{MgCl}_2$ , 120 mM KCl, 5 mM potassium oxalate, 0.1 mM EGTA, 0.1 mM  $^{45}\text{CaCl}_2$  and 25  $\mu$ M ruthenium red. Ruthenium red was added as an inhibitor of the  $\text{Ca}^{2+}$  release channel. The reaction was initiated by adding SR vesicles (2 mg/ml protein) to the reaction mixture at 37°C and terminated after 1 min by filtration. The filters were washed, dried and counted using a Liquid Scintillation System LS 1701 from Beckman.

#### **Western blot analysis**

The protein content of SR  $\text{Ca}^{2+}$ -cycling proteins SERCA2a, PLB and its phosphorylated forms Ser16-PLB and Thr17-PLB was determined by Western blot analysis as described previously (221-225). Protein samples (1 mg/ml of SR) were separated by sodium dodecyl sulfate-polyacrylamide gel electrophoresis (SDS-PAGE) and transferred to polyvinylidene difluoride (PVDF) membranes. PVDF membranes were probed with a monoclonal anti-SERCA2a antibody obtained from Affinity Bioreagents Inc. (Golden, CO), monoclonal anti-PLB antibody obtained from Upstate Biotechnology (Lake Placid, NY), polyclonal anti-Ser16-PLB and polyclonal anti-Thr17-PLB obtained from Badrilla (Leeds, UK). Appropriate secondary antibodies were used, and the antibody-antigen complexes in all membranes were detected using an ECL kit from

Amersham (Buckinghamshire, UK). GAPDH was used as a loading control. An Imaging Densitometer model GS-800 from Bio-Rad Ltd. (Hercules, CA) was used to scan the protein bands which were quantified using the Quantity One 4.5.0 software. Background subtraction was achieved by reading the absorbance of an equally sized area adjacent to the band. In the cases where data were generated from samples placed on multiple gels, one sample was chosen as a reference and loaded onto each gel. The absorbances of the samples were adjusted according to the intensity of the reference sample band.

### **Measurement of SR-associated CaMKII and PKA activities**

CaMKII and PKA activities were measured using Upstate Biotechnology (Lake Placid, NY) assay kits as described previously (221-225). The assay kit for CaMKII activity is based on the phosphorylation of a specific substrate, autocalmitide, and measures the transfer of the  $\gamma$ -phosphate of [ $\gamma$ - $^{32}$ P] ATP by CaMKII. The assay kit for PKA activity measurement is based on the phosphorylation of a specific substrate, kemptide, after transfer of the  $\gamma$ -phosphate of [ $\gamma$ - $^{32}$ P] ATP by PKA. The reactions for CaMKII and PKA were started by adding [ $\gamma$ - $^{32}$ P] ATP to the reaction mixture containing 1 mg/ml of SR, the respective assay dilution buffers, substrates and inhibitor cocktails (all provided in the kits) and after incubating for 10 min at 30°C the reaction was stopped by spotting the reaction mixture onto phosphocellulose filter papers. Subsequently, the filters were washed three times with phosphoric acid and once with acetone and counted using a Liquid Scintillation System LS 1701 from Beckman. The activities of CaMKII and PKA were calculated as the difference between values obtained in the presence and absence of the exogenous substrate.

### **Measurement of SR-associated protein phosphatase activity**

The measurement of SR-associated protein phosphatase (PP) activity was based on a technique established previously (221,222,225,227) using the Serine/Threonine assay kit obtained from Upstate Biotechnology (Lake Placid, NY). This assay is based upon the principle of dephosphorylation of the synthetic phosphopeptide KRpTIRR. The reaction was initiated by the addition of 2.4 mg/ml of SR to a microtiter well in the presence or absence of the synthetic substrate (200  $\mu$ M) and incubated for a period of 30 min at room temperature. Termination of the reaction was achieved by the addition of Malachite Green solution, and the absorbance was read after 15 min at 650 nm to determine the amount of inorganic phosphate released.

### **Statistical analysis**

Values are expressed as mean  $\pm$  standard error (S.E.). One way analysis of variance (ANOVA) was used to analyze variations between the means of groups. Significant values versus sham controls are defined as  $P < 0.05$ .

## V. RESULTS

### **General characteristics of rats subjected to 2, 4, 16 and 28 weeks of pressure overload (PO) or volume overload (VO).**

The general characteristics of PO and VO rats are depicted in Tables 1 and 2. In this study, heart-to-body weight (HBW) ratio was calculated and used as an index of cardiac hypertrophy. As shown in Table 1 and Table 2, the HBW ratio was observed to be significantly increased in rats subjected to PO or VO compared to sham controls at all time points. Body weight of the animals remained relatively constant throughout the study except for 16 week VO group which was slightly but significantly elevated compared to its sham operated group (Table 2). There were no major differences between the sham groups of the PO and VO studies, except body weight, which was slightly but significantly higher in the 4-week sham group from the VO study.

The organ wet-to-dry ratio determines the presence of congestion which is a marker of heart failure. The ratio of wet-to-dry liver in PO and VO rats remained unchanged throughout the study while congestion was observed in the lungs only at 28 weeks in the VO model (Tables 1 and 2). Abdominal fluid build-up/ascites (another marker of congestion/heart failure) was not observed at any time point in either experimental model during the course of the study (Tables 1 and 2).

### **Echocardiographic analysis of cardiac structure/function in rats subjected to 2, 4, 16 and 28 weeks of pressure overload (PO) or volume overload (VO).**

Table 3 and Table 4 include a series of measurements of LV parameters *in vivo*, such as LV structure at systole and diastole as well as diastolic and systolic function of the LV in PO and VO, respectively, as obtained by utilizing 2-D guided M-Mode

echocardiography and Doppler wave measurements. To examine whether cardiac contractile dysfunction occurred in PO or VO animals, *in vivo* cardiac performance was assessed by echocardiography. Heart rate in PO animals was significantly higher at 16 weeks and 28 weeks following the surgery compared to the corresponding sham operated controls (Table 3). Throughout the course of the study, the heart rate in VO animals did not change significantly compared to their respective control group (Table 4). Ejection fraction (EF) refers to the fraction of the end diastolic volume pumped out of a ventricle with each heart beat and is a measure of the systolic function. The percent fractional shortening (%FS) is also a measure of the systolic function and is defined as the ratio of the difference between the end-diastolic and end-systolic LV dimension divided by the end-diastolic dimension. The %FS and EF were reduced at 16 and 28 weeks in VO animals (Table 4). Approximately the same degree of the reduction was observed at the two time points. In contrast, in PO, the impairment of systolic function was observed only at 28 weeks, as evident by the significant reduction in %FS (Table 3). The rats subjected to VO exhibited significant increase in cardiac output (CO) at all time points; the output was more prominent at 16 and 28 weeks, with approximately a 2-fold increase compared to sham group. CO in PO rats was elevated only at 28 weeks. There were no statistically significant differences between the sham groups of the PO and VO studies, with the exception of CO, which was elevated in the 4-week sham group from the VO study.

The time that is needed for the heart to relax following the end of one contractile phase and the beginning of a new one is termed IVRt and is used as a measure of the diastolic function. Table 4 shows significantly reduced IVRt in rats subjected to VO

when compared to their sham controls at all time points. The reduction was similar at all time points. The rats subjected to PO exhibited significantly prolonged IVRt at 4 weeks and subsequent time points (Table 3). The extent of increase in the IVRt in PO rats was similar at 4, 16 and 28 weeks.

In this study echocardiography was also used to monitor the changes in LV structure during the progression of PO- or VO-induced hypertrophy. The left ventricular internal dimension (LVID), left ventricular posterior wall thickness (LVPW) and interventricular septal wall thickness (IVS) were evaluated for each time point, at both systole and diastole (Tables 3 and 4). PO rats exhibited prominent increase in IVS and LVPW at systole and diastole at all time points in the study; however LVID was slightly increased only after 28 weeks. In contrast, in VO rats there was a significant increase in LVID at all time points when compared to sham operated rats. The thickness of the LV walls remained unchanged in VO rats for the most part except at 28 weeks where the walls exhibited significant thickening.

#### **SR $\text{Ca}^{2+}$ -uptake.**

Alterations in diastolic function of the heart could in major part be linked to abnormalities in SR  $\text{Ca}^{2+}$ -uptake. Figure 1A-D shows SR  $\text{Ca}^{2+}$ -uptake measurements taken at 2, 4, 16 and 28 weeks for both PO and VO groups. In PO animals  $\text{Ca}^{2+}$ -uptake was unchanged compared to control group at 2 weeks following the surgery (Fig. 1A). At 4 and 16 weeks  $\text{Ca}^{2+}$ -uptake was found to be significantly elevated in PO rats compared to the sham operated group (39% and 67%, respectively) (Fig. 1B and C). At 28 weeks, the uptake was not significantly different between PO rats and control (Fig. 1D). In the rats subjected to VO,  $\text{Ca}^{2+}$ -uptake was unchanged compared to the control group at 2 and

4 weeks following the surgery (Fig. 1A and B). At 16 and 28 weeks VO rats exhibited significant increase in  $\text{Ca}^{2+}$ -uptake (76% and 52%, respectively) compared to the control group (Fig. 1C and D).

#### **Protein levels of SERCA, PLB, Ser16-PLB and Thr17-PLB.**

Changes in SR  $\text{Ca}^{2+}$ -uptake may be directly linked to the protein levels of SERCA2a and its negative regulator phospholamban (PLB) as well as the phosphorylation status of PLB. Western blot analysis was used to examine the protein level of SERCA2a as well as PLB and its phosphorylated forms (Ser16-PLB and Thr17-PLB) at 16 weeks (Fig. 2) and 28 weeks (Fig. 3) – time points when alterations in SR  $\text{Ca}^{2+}$ -uptake were observed in both experimental models – in PO and VO rats. In the PO group, the levels of SERCA2a were found to be significantly increased by 212% at 16 weeks compared to sham operated animals (Fig. 2A). SERCA2a expression was not found to be significantly different in PO rats versus sham control at 28 weeks (Fig. 3A). The levels of PLB were found to be unaltered in PO rats at 16 and 28 weeks when compared to their respective controls (Fig. 2B, Fig. 3B). The levels of SERCA2a were significantly increased in VO rats at 16 weeks (103% increase) compared to sham (Fig. 2A). At 28 weeks there was no significant difference between VO and control with respect to SERCA2a levels (Fig.3A). The levels of PLB in VO rats did not differ significantly when compared to control at 16 and 28 weeks (Fig. 2B, Fig. 3B).

Figure 2C and Figure 2D show a significant increase in Ser16-PLB and Thr17-PLB in PO rats at 16 weeks (1.84-fold vs. sham and 1.55-fold vs. sham, respectively). In VO rats, Ser16-PLB was significantly reduced by approximately 42.4% compared to control at 16 weeks (Fig. 2C) while the level of Thr17-PLB was found unaltered at this



time point (Fig. 2D). As shown in Fig. 3C and D, at 28 weeks, Ser16-PLB and Thr17-PLB were reduced in PO rats by a significant 63% and 79%, respectively, compared to controls. The levels of Ser16-PLB and Thr17-PLB were found to be significantly reduced by 69% at 28 weeks in VO rats relative to their respective control groups (Fig. 3C and D).

#### **The activities of SR-associated PKA, CaMKII and phosphatases.**

The phosphorylation status of PLB has been associated with alterations in the activities of SR-associated kinases, such as PKA, CaMKII, and protein phosphatases. The activities of kinases and phosphatases, shown in Fig. 4 and Fig. 5, respectively, were examined at the 28-week time point (time point when phosphorylation of PLB was reduced in both models). SR-associated PKA activity was found to be unaltered between PO rats and control group (Fig. 4A). As shown in Figure 4B, SR-associated CaMKII activity was significantly increased in PO animals (16.3% vs. sham). The phosphatase activity shown in Fig. 5 represents the total SR-associated phosphatase activity. SR-associated phosphatase activity in PO animals was found to be significantly higher compared to sham operated rats (1.59-fold vs. sham). As shown in Fig. 4A and 4B, VO rats exhibited a significant reduction in the activities of PKA and CaMK compared to control (29% decrease vs. sham and 26% decrease vs. sham, respectively). Figure 5 indicates a significant increase in the activities of phosphatases in VO when compared to sham-operated rats (1.48-fold vs. sham).

Table 1. General characteristics of rats subjected to pressure overload (PO).

	2 weeks		4 weeks		16 weeks		28 weeks	
Parameter	Sham (n=6-7)	PO (n=6-8)	Sham (n=8)	PO (n=12-15)	Sham (n=9)	PO (n=15-17)	Sham (n=6-11)	PO (n=6-9)
Heart Weight (g)	0.94± 0.04	1.27± 0.05*	1.17± 0.03	1.44± 0.05*	1.42± 0.04	2.00± 0.06*	1.57± 0.03	2.11± 0.11*
Body Weight (g)	262.3± 3.2	276.5± 10.1	385.5± 11.7	364.3± 7.1	609.9± 10.7	600.6± 11.3	694.9± 17.6	715.9± 20.6
HBW ratio (mg/100g)	359.3± 15.7	486.8± 29.4*	302.6± 4.2	383.5± 11.8*	232.4± 5.3	334.5± 10.2*	216.1± 6.4	288.4± 8.9*
Lungs Wet/Dry	4.39± 0.08	4.56± 0.05	4.23± 0.04	4.30± 0.03	3.85± 0.04	3.84± 0.05	3.91± 0.04	3.84± 0.07
Liver Wet/Dry	2.85± 0.01	2.88± 0.02	2.80± 0.03	2.87± 0.03	2.78± 0.02	2.75± 0.02	2.63± 0.04	2.80± 0.05
Ascites	-	-	-	-	-	-	-	-

The mortality rate associated with the aortic banding procedure was 26%. Results are expressed as means ± SE. Statistically significant differences (indicated with an asterisk, \*) between sham operated and PO animals were determined by one-way ANOVA ( $P < 0.05$ ).

Table 2. General characteristics of rats subjected to volume overload (VO).

	2 weeks		4 weeks		16 weeks		28 weeks	
Parameter	Sham (n=5-6)	VO (n=6-10)	Sham (n=6-8)	VO (n=11-24)	Sham (n=10-13)	VO (n=11-14)	Sham (n=21-28)	VO (n=19-29)
Heart Weight (g)	0.95± 0.03	1.43± 0.05*	1.24± 0.03	1.83± 0.06*	1.42± 0.04	2.47± 0.12*	1.65± 0.03	2.84± 0.15*
Body Weight (g)	284.3± 4.5	286.6± 7.32	423.8± 9.0	402.8± 6.0	595.1± 9.5	635.0± 15.0*	761.8± 17.4	782.6± 17.4
HBW ratio (mg/100g)	332.9± 9.3	482.1± 17.2*	284.9± 4.9*	459.8± 14.8*	238.9± 2.5	399.2± 21.7*	216.2± 2.7	362.5± 16.7*
Lungs Wet/Dry	4.67± 0.15	4.44± 0.03	4.00± 0.07	4.10± 0.06	3.78± 0.05	3.87± 0.04	4.01± 0.04	4.35± 0.05*
Liver Wet/Dry	2.96± 0.09	2.94± 0.02	2.71± 0.01	2.76± 0.02	2.79± 0.02	2.79± 0.03	2.81± 0.03	2.88± 0.03
Ascites	-	-	-	-	-	-	-	-

The mortality rate associated with the aortocaval shunt procedure was 7%. Results are expressed as means ± SE. Statistically significant differences (indicated with an asterisk, \*) between sham operated and VO animals were determined by one-way ANOVA ( $P < 0.05$ ).

Table 3. Echocardiographic parameters of cardiac function and structure in rats subjected to 2, 4, 16 and 28 weeks of pressure overload (PO).

	2 weeks		4 weeks		16 weeks		28 weeks	
Parameter	Sham (n=13-17)	PO (n=19-23)	Sham (n=25-28)	PO (n=30-38)	Sham (n=14-18)	PO (n=15-18)	Sham (n=17-20)	PO (n=12-22)
Heart rate (bpm)	385.6± 8.9	381.8± 6.5	353.0± 4.6	364.2± 4.2	331.3± 5.1	350.1± 6.0*	315.9± 2.5	340.3± 4.2*
FS (%)	43.98± 0.77	42.97± 1.00	41.82± 0.96	43.15± 1.10	42.38± 0.95	41.33± 1.53	44.10± 0.69	40.51± 1.18*
EF	0.802± 0.008	0.790± 0.010	0.772± 0.011	0.777± 0.012	0.782± 0.010	0.768± 0.018	0.788± 0.010	0.775± 0.015
CO (ml/min)	279.2± 14.6	272.5± 12.3	297± 13.2	294.3± 14.0	0.369± 0.020	0.409± 0.024	0.464± 0.017	0.574± 0.031*
IVRt (ms)	22.5± 0.9	23.8± 0.6	20.9± 0.7	24.5± 0.6*	22.2± 0.8	26.2± 0.7*	24.1± 0.5	28.3± 0.5*
LVIDd (cm)	0.737± 0.015	0.733± 0.014	0.772± 0.013	0.754± 0.013	0.908± 0.014	0.936± 0.021	0.969± 0.014	0.997± 0.019
LVIDs (cm)	0.407± 0.012	0.427± 0.014	0.457± 0.009	0.468± 0.013	0.511± 0.014	0.563± 0.023	0.542± 0.014	0.598± 0.013*
IVSd (cm)	0.146± 0.006	0.184± 0.005*	0.162± 0.005	0.211± 0.006*	0.183± 0.010	0.222± 0.008*	0.155± 0.005	0.211± 0.010*
IVSs (cm)	0.252± 0.007	0.306± 0.007*	0.261± 0.007	0.330± 0.006*	0.300± 0.009	0.339± 0.008*	0.295± 0.007	0.353± 0.010*
LVPWd (cm)	0.145± 0.006	0.205± 0.007*	0.155± 0.006	0.215± 0.007*	0.167± 0.009	0.224± 0.008*	0.165± 0.004	0.220± 0.009*
LVPWs (cm)	0.256± 0.008	0.321± 0.008*	0.254± 0.005	0.332± 0.008*	0.289± 0.008	0.356± 0.011*	0.301± 0.005	0.358± 0.007*

Results are expressed as means ± SE. Statistically significant differences (indicated with an asterisk, \*) between sham operated and PO animals were determined by one-way ANOVA (P < 0.05).

Table 4. Echocardiographic parameters of cardiac function and structure in rats subjected to 2, 4, 16 and 28 weeks of volume overload (VO).

	2 weeks		4 weeks		16 weeks		28 weeks	
Parameter	Sham (n=9-15)	VO (n=24-30)	Sham (n=8-14)	VO (n=18-28)	Sham (n=13-18)	VO (n=15-17)	Sham (n=13-18)	VO (n=11-19)
Heart rate (bpm)	363.1± 6.8	373.2± 3.0	335.3± 5.0	344.7± 4.1	318.7± 5.4	322.8± 5.8	313.0± 3.5	323.3± 4.5
FS (%)	43.37± 1.32	44.02± 0.82	42.95± 1.53	42.49± 1.20	42.45± 1.37	37.50± 0.88*	44.77± 1.15	37.69± 0.78*
EF	0.793± 0.013	0.797± 0.009	0.786± 0.015	0.777± 0.012	0.787± 0.016	0.731± 0.008*	0.807± 0.013	0.721± 0.009*
CO (ml/min)	302.7± 18.7	513.8± 22.6*	352.9± 15.9	659.6± 36.9*	0.395± 0.032	0.828± 0.049*	0.478± 0.025	0.974± 0.035*
IVRt (ms)	22.1± 0.6	18.4± 0.6*	21.5± 0.7	17.6± 0.6*	21.1± 0.5	18.6± 0.6*	23.5± 0.5	20.9± 0.6*
LVIDd (cm)	0.778± 0.017	0.920± 0.016*	0.825± 0.029	1.015± 0.021*	0.943± 0.027	1.214± 0.030*	0.986± 0.019	1.284± 0.016*
LVIDs (cm)	0.440± 0.013	0.500± 0.011*	0.489± 0.015	0.587± 0.013*	0.544± 0.022	0.770± 0.022*	0.518± 0.018	0.820± 0.011*
IVSd (cm)	0.153± 0.006	0.143± 0.005	0.154± 0.009	0.153± 0.005	0.164± 0.009	0.159± 0.010	0.157± 0.006	0.181± 0.005*
IVSs (cm)	0.277± 0.013	0.267± 0.006	0.262± 0.008	0.276± 0.007	0.287± 0.009	0.281± 0.011	0.300± 0.012	0.356± 0.011*
LVPWd (cm)	0.150± 0.007	0.146± 0.004	0.142± 0.008	0.158± 0.004	0.167± 0.007	0.187± 0.007	0.162± 0.004	0.233± 0.006*
LVPWs (cm)	0.265± 0.010	0.275± 0.005	0.257± 0.008	0.285± 0.007*	0.288± 0.011	0.309± 0.007	0.301± 0.008	0.354± 0.009*

Results are expressed as means ± SE. Statistically significant differences (indicated with an asterisk, \*) between sham operated and VO animals were determined by one-way ANOVA (P < 0.05).

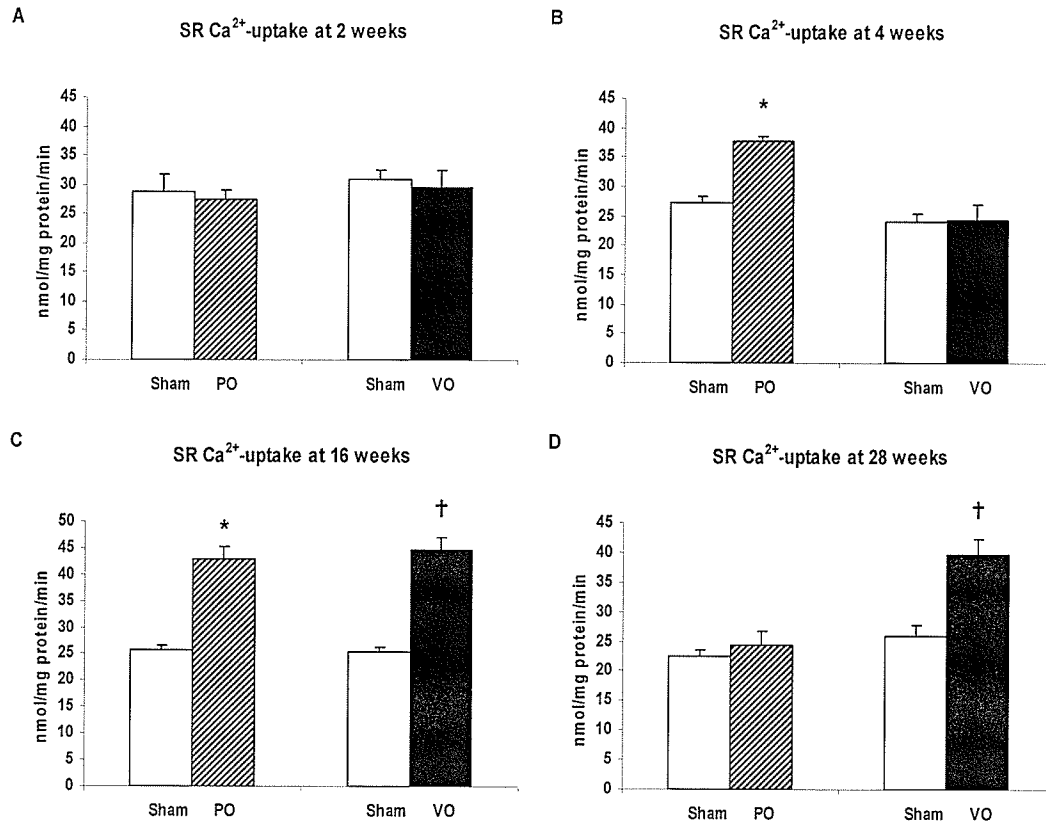


Figure 1. SR  $\text{Ca}^{2+}$  uptake in 2-week (panel A), 4-week (panel B), 16-week (panel C) and 28-week (panel D) pressure overload (PO) and volume overload (VO) rats. The n values are given for each group at 2, 4, 16 and 28 weeks in sequential order: Sham PO (5,5,4,9); PO (3,5,6,9); Sham VO (3,4,6,5); VO (3,4,9,5). The data are presented as means  $\pm$  SE. Statistically significant differences ( $P < 0.05$ ) between sham operated controls and PO samples are indicated (\*), as are the differences between sham operated controls and VO samples (†). One-way ANOVA was used to analyze variations between the means of groups.

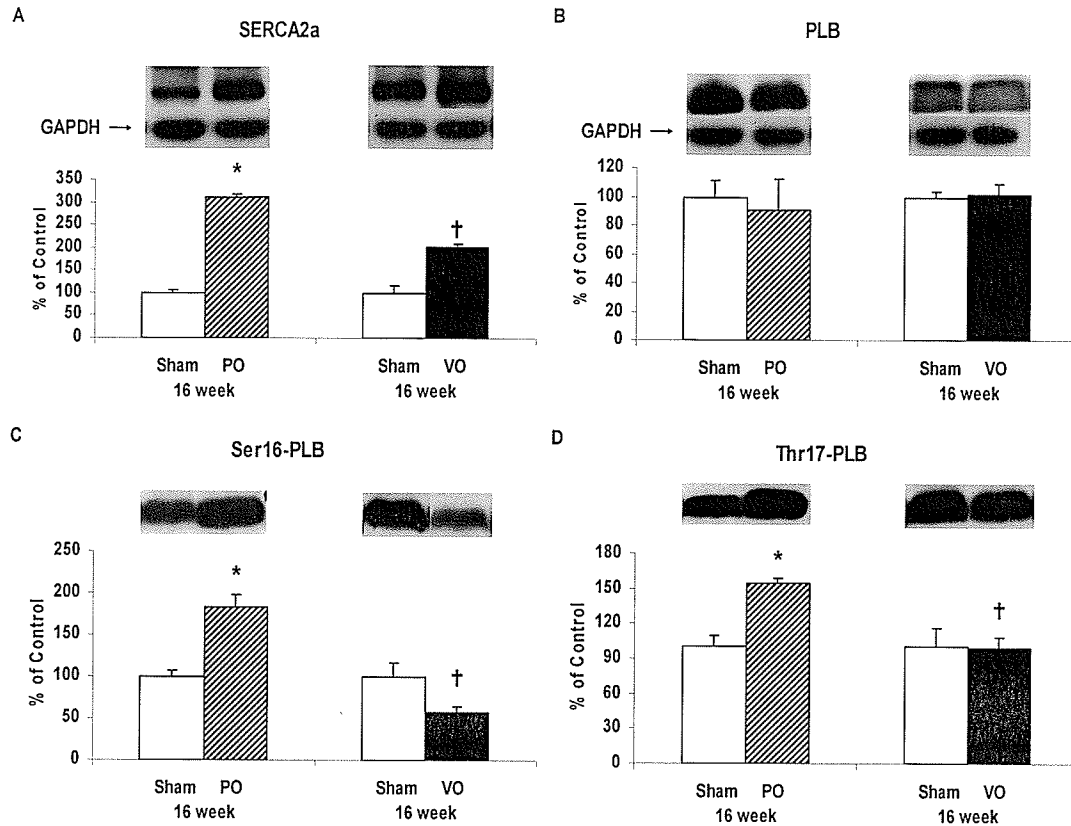


Figure 2. Western blot analysis of sarco/endoplasmic reticulum  $\text{Ca}^{2+}$ -ATPase (SERCA2a) (panel A), phospholamban (PLB) (panel B), Ser16 phosphorylated phospholamban (Ser16-PLB) (panel C) and Thr17 phosphorylated phospholamban (Thr17-PLB) (panel D) in 16-week pressure overload (PO) and volume overload (VO) rats. The n values in panels A-D are given in sequential order: Sham PO (4,4,6,4); PO (6,3,5,4); Sham VO (5,7,5,4); VO (7,7,4,4). The absorbance of sham operated controls was set to 100%. The data are presented as means  $\pm$  SE. Statistically significant differences ( $P < 0.05$ ) between sham operated controls and PO samples are indicated (\*), as are the differences between sham operated controls and VO samples (†). One-way ANOVA was used to analyze variations between the means of groups.

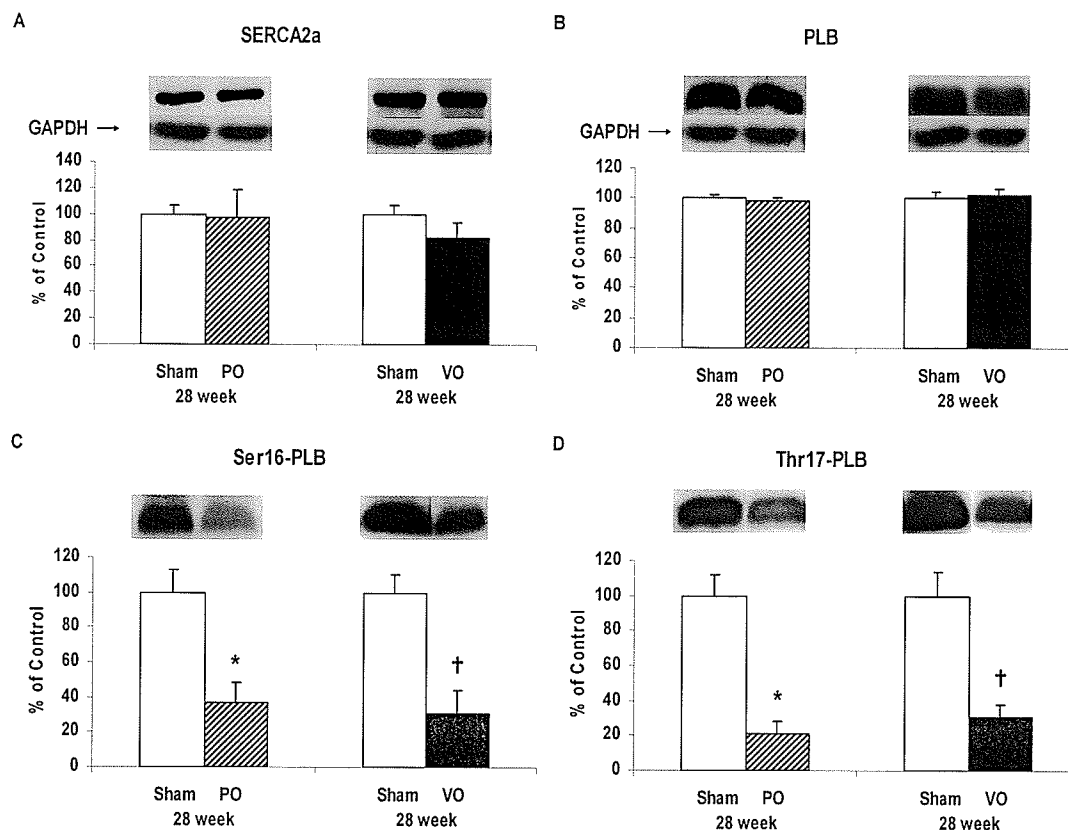


Figure 3. Western blot analysis of sarco/endoplasmic reticulum  $\text{Ca}^{2+}$ -ATPase (SERCA2a) (panel A), phospholamban (PLB) (panel B), Ser16 phosphorylated phospholamban (Ser16-PLB) (panel C) and Thr17 phosphorylated phospholamban (Thr17-PLB) (panel D) in 28-week pressure overload (PO) and volume overload (VO) rats. The n values in panels A-D are given in sequential order: Sham PO (5,7,6,5); PO (4,6,6,6); Sham VO (5,7,5,5); VO (5,7,4,6). The absorbance of sham operated controls was set to 100%. The data are presented as means  $\pm$  SE. Statistically significant differences ( $P < 0.05$ ) between sham operated controls and PO samples are indicated (\*), as are the differences between sham operated controls and VO samples ( $\dagger$ ). One-way ANOVA was used to analyze variations between the means of groups.



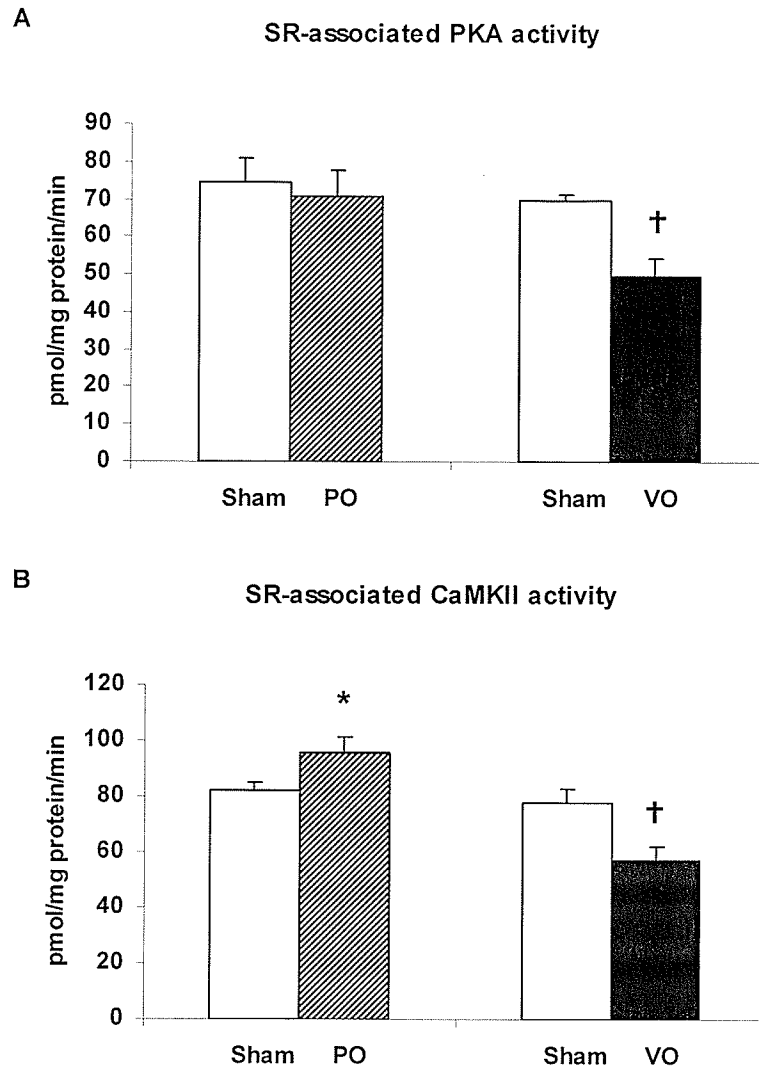


Figure 4. SR-associated cyclic AMP-dependent protein kinase (PKA) activity (panel A) and  $\text{Ca}^{2+}$ /calmodulin-dependent protein kinase II (CaMKII) activity (panel B) in 28-week pressure overload (PO) and volume overload (VO) rats. The n values in panels A and B are given in sequential order: Sham PO (5,7); PO (5,4); Sham VO (4,5); VO (4,4). The data are presented as means  $\pm$  SE. Statistically significant differences ( $P < 0.05$ ) between sham operated controls and PO samples are indicated (\*), as are the differences between sham operated controls and VO samples (†). One-way ANOVA was used to analyze variations between the means of groups.

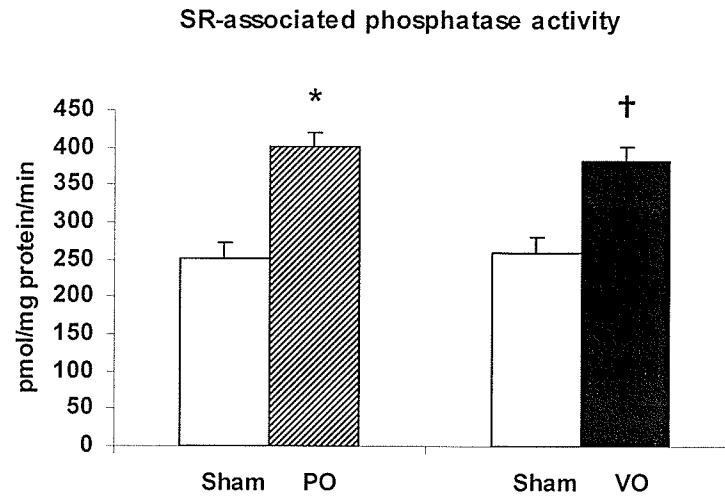


Figure 5. SR-associated protein phosphatase (PP) activity in 28-week pressure overload (PO) and volume overload (VO) rats. The n values are given in sequential order: Sham PO (5); PO (4); Sham VO (6); VO (6). The data are presented as means  $\pm$  SE. Statistically significant differences ( $P < 0.05$ ) between sham operated controls and PO samples are indicated (\*), as are the differences between sham operated controls and VO samples (†). One-way ANOVA was used to analyze variations between the means of groups.

## VI. DISCUSSION

This study is the first of its kind to assess the etiology-specific differences between PO and VO hearts, their function and their association with changes in the status of the SR over an identical time course in the same animal species. Echocardiographic changes in left ventricular geometry and performance in PO and VO models of cardiac hypertrophy have been previously documented (184,185,199,207,227). However, there is scattered, inconsistent and limited information in the literature regarding the status of the SR and its contribution to contractile abnormalities caused by hypertrophy due to chronic PO or VO. A few studies have performed short time course comparative analysis (227) or single time-point comparisons of cardiac performance in PO versus VO (228,229); however, the status of the SR was not examined. We have therefore conducted a carefully designed, detailed analysis of cardiac performance and SR function as well as its regulation over an elaborate time course entailing the progression of cardiac hypertrophy due to PO as well as VO.

### **Basic characteristics**

Both PO and VO resulted in cardiac hypertrophy which developed as early as 2 weeks and persisted throughout the 28-week course of the study (Table 1, Table 2). It has been well established that cardiac hypertrophy, although adaptive in response to hemodynamic stress, proceeds to heart failure if prolonged (1,37). Some signs of overt heart failure were visible in the advanced stages of hypertrophy. A slight, but significant pulmonary congestion was observed at 28 weeks only in the rats subjected to VO indicating that the condition in this group progressed to pre-heart failure stage. With regards to VO, the difference in results between other reports and our study could be attributed to the species

specific response to the stimuli, the age of the animals at the time of induction of VO, the size of the aortocaval (AV) shunt and methods of measurement of heart function (163,250). Ohkusa et al. (230) observed no signs of severe heart failure 10 months after the induction of PO by abdominal aortic banding (AAB) in male Wistar rats. Gupta et al. (203) on the other hand reported the presence of pulmonary congestion, and thus overt heart failure in Lewis rats after 8 weeks of PO induced by one-kidney, one-clip (1K1C) procedure. The earlier onset of heart failure in this study was likely due to the use of a different rat species and a dissimilar technique for achieving PO on the left ventricle as compared to the ones used by Ohkusa et al. (230). Heart failure was also reported at the 27-week time point in Sprague-Dawley rats (185) and at the 19-23 weeks in Wistar rats (184) subjected to PO; in these studies, the PO on the heart was achieved by constricting ascending portion of the aorta and thus placing more severe load on the heart compared to our model wherein the occlusion was placed more distal (descending aorta in abdominal region). This might be one of the reasons why in our case hypertrophy did not progress to heart failure after 28 weeks of PO.

### **Heart structure**

Echocardiographic analysis of LV structure revealed morphological difference between the hearts subjected to PO or VO. In this study, the rat hearts subjected to PO remodeled in a typical concentric fashion as expected. Conversely, VO rats for most part showed evidence of pure eccentric hypertrophy. Rat hearts subjected to VO remodeled in eccentric fashion which is characterized by the enlargement of LV internal dimensions without notable wall thickening and is reported elsewhere in the setting of VO (56,199,231). At 28 weeks, however, as shown in Table 4, the LV walls in VO hearts

became significantly thicker. This could be due to more extensive hypertrophy in VO compared to PO hearts (Table 1, Table 2), as indicated by higher HBW ratios for VO rats. In our VO model, PO may be also involved as the extra blood (that is shunted back to the heart) is being pumped out into high pressure systemic circulation. This would in turn increase systolic pressure resulting in PO on the heart (214,232). Whether this is the case in our model is unknown, however, the increase in thickness that we observed at 28 weeks seems to indicate that PO may be a factor in our model of cardiac hypertrophy. The enlargement of hearts in PO rats is primarily due to the walls becoming thicker, whereas in VO rats, the enlargement is primarily, as already stated, due to increase in the LV chamber size and in this case with LV wall thickening also contributing (at later stages). Cardiac structure in our models was consistent with other comparable studies that subjected animals to PO (47,184,185,199) and/or VO (199,207) over a long time course.

### **Heart function**

Although very few studies of cardiac hypertrophy in animal models of PO or VO have assessed diastolic dysfunction, our findings are consistent with the studies conducted to date (199,233). Diastolic dysfunction, including a prolonged IVRt, LV wall thickening and the absence of dilatation, was reported in PO Wistar rats throughout the course of 4-12 weeks study (233). Likewise, our study has shown that PO and resulting concentric remodeling was associated with early diastolic dysfunction. Also, the IVRt interval was prolonged at 4 weeks onwards, which is consistent with findings published earlier (199). It is well known that hypertrophy due to PO generally induces fibrosis of cardiac tissue (59,234-237), which we feel may be responsible for impaired left ventricular relaxation. Diastolic dysfunction is frequently observed upon assessment of

patients with endomyocardial fibrosis and in animal models that mimic the condition (234,236-238).

In contrast, VO-induced cardiac hypertrophy was associated with improved diastolic function, as indicated by the reduced IVRt interval, which is consistent with a previous study of chronic VO (199). One of the striking features of the VO heart was a prominent elevation in cardiac output, which is of course the consequence of a larger volume of blood being shunted back to the heart - this being an example of a compensatory mechanism aimed at ensuring continuous and adequate blood delivery to the periphery in the face of increased preload on the heart. Conversely, fibrosis in VO typically does not occur. Therefore, with enhanced venous return and dilatation of the left ventricle, enhanced diastolic function should be expected in the compensatory stage of VO.

Whether systolic dysfunction is evident in hypertrophic animal models is controversial and disputed. Some studies of PO showed enhanced systolic function in early stages of hypertrophy, followed by a progression into failing stages and subsequent systolic dysfunction (184). The enhancement of systolic and diastolic function has been reported in male Wistar rats subjected to 10 days, 4 weeks and 8 weeks of PO (230). In contrast, Müller et al. (239) demonstrated both systolic and diastolic dysfunction in rats subjected to 10 weeks of PO. Furthermore De Stefano et al. (240) also showed systolic and diastolic dysfunction in their 20-week old rats subjected to 8 weeks of VO (induced by AV shunt). De Stefano et al. (240) noted no signs of overt heart failure in their animals which they attributed to increased LV compliance as a consequence of eccentric remodeling and chamber dilatation. In a dog model of VO (induced by A-V block) one

group showed impairment of diastolic function with no abnormalities in systolic function with the progression of eccentric remodeling (213).

Our study, however, showed that in PO the signs of systolic dysfunction became evident only at 28 weeks when the %FS was found to be significantly reduced. Increased heart rate and cardiac output at 28 weeks developed perhaps as a late stage compensatory mechanism directed towards counteracting systolic and diastolic dysfunction and progression into heart failure and ensuring adequate blood perfusion of tissues and organs. Systolic dysfunction in VO became apparent at 16 weeks and continued until 28 weeks as evidenced by a significant reduction in both EF and %FS. The absence of systolic dysfunction prior to 16 weeks is in agreement with the study by Dudas Gyorki et al. (241) who showed no systolic impairment in dogs subjected to 12 weeks of VO. The absence of systolic dysfunction at 4 weeks is in general agreement with Hashida et al. (208) who reported normal fractional shortening 3 weeks following AV shunt creation. Although we observed significant systolic dysfunction at 16 weeks into the study, we are not sure when systolic impairment starts to occur in our rats. Even though both PO and VO led to the development of systolic dysfunction, the dysfunction was more prominent in VO model. The larger extent of systolic impairment might in part explain the slight but significant pulmonary congestion observed in animals subjected to VO at 28 weeks. Systolic dysfunction would compromise the heart's ability to pump blood out into the systemic circulation resulting in pooling of the blood in other places such as the lungs. Our study shows that despite not being in overt failure stages, both PO and VO models exhibit significant systolic dysfunction. We believe that this systolic dysfunction (in PO) is a secondary response to the aforementioned diastolic dysfunction that begins much

earlier in the time course. On the other hand, systolic dysfunction in VO is likely an independent response, as diastolic function in VO is enhanced at all time points.

These data suggest that 28 weeks of PO or VO in rats induces compensatory hypertrophic responses, albeit differential in nature, as supported by the etiology-specific alterations in left ventricular geometry and performance. Some signs of overt heart failure were visible in the advanced stages of hypertrophy in the VO model but not in PO rats. In the current study, our results on cardiac structure and function are generally in agreement with our previous report (199).

#### **Association between SR $\text{Ca}^{2+}$ -uptake & cardiac function**

Cardiac dysfunction, systolic or diastolic, observed in various types of cardiac pathologies has been attributed in part to impaired  $\text{Ca}^{2+}$  handling by the SR, the largest intracellular store of  $\text{Ca}^{2+}$ . In this study, one of our goals was to establish the role of the SR in the regulation of cardiac function during the progression of PO- or VO-induced left ventricular hypertrophy (LVH).

In early stage LVH, namely at 2 and 4 weeks, there was no clear-cut association between SR function and cardiac function in PO or VO. Although at 2 weeks, in PO hearts,  $\text{Ca}^{2+}$ -uptake was unaltered with systolic and diastolic function being preserved, which was as expected, 4-week PO rats, however, exhibited diastolic impairment in spite of elevated  $\text{Ca}^{2+}$ -uptake. If SR function is elevated, what counteracts it to depress diastolic function in the early, 4-week stage of PO? The presence of fibrosis, which is known to occur in PO, results in a stiffer chamber possibly outweighing the benefits of hyperfunctional SR and thus leading to diastolic impairment. However, several studies have shown that the functional alterations at the level of the SR (i.e. elevated  $\text{Ca}^{2+}$ -



uptake) might be a part of the compensatory hypertrophic response to hemodynamic overload (203,230,242-244). In other words, elevated  $\text{Ca}^{2+}$ -uptake, we speculate, may be an important mechanism for preventing further deterioration of diastolic function at the early stages of PO.

In 2- and 4-week VO rats, systolic function was preserved as well; however, the improvement in diastolic function, as evident from shortened IVRt interval, did not correlate with  $\text{Ca}^{2+}$ -uptake which was unaltered. If the SR function is normal, what else could have an effect on improving cardiac relaxation in the early stages of VO? Since SR  $\text{Ca}^{2+}$ -uptake was unaltered at the 4-week time point, improved diastolic function could be attributed to the other major determinant of relaxation, the sodium-calcium exchanger (NCX) and sarcolemmal  $\text{Ca}^{2+}$ -ATPase, or other processes, such as activity and concentration of  $\text{Ca}^{2+}$  ligands that remove cytosolic  $\text{Ca}^{2+}$  (54,101,102,245). However, the status of the NCX and other relevant  $\text{Ca}^{2+}$  binding proteins which could aid in relaxation were outside the scope of the current investigation.

At the 16-week time point both PO and VO exhibited a similar increase in  $\text{Ca}^{2+}$ -uptake. Sixteen-week VO rats exhibited a significant increase in  $\text{Ca}^{2+}$ -uptake, which was associated with the observed improvement in diastolic function (decreased IVRt). The elevation in SR  $\text{Ca}^{2+}$ -uptake may be a compensatory mechanism for preventing the transition from compensatory hypertrophy to the decompensatory stage of cardiac hypertrophy. Increased SR  $\text{Ca}^{2+}$ -uptake in 16-week VO rats was consistent with an increase in the protein level of SERCA2a. Since phosphorylation of PLB at Ser16 and Thr17 relieves the inhibitory action of PLB on SERCA2a, and stimulates SR  $\text{Ca}^{2+}$ -uptake (108), it was surprising to observe a reduction in Ser16-PLB phosphorylation in 16-week

VO hearts; Thr17-PLB was unaffected. Thus, it is possible that there may be other mechanisms which have offset the reduction in Ser16-PLB phosphorylation. In VO, despite the decreased Ser16-PLB and unaltered Thr17-PLB phosphorylation, which would favor a reduction in  $\text{Ca}^{2+}$ -uptake, the elevation observed was probably due to an increase in SERCA2a levels as documented in Fig. 2A.

Sixteen-week PO rats failed to demonstrate improvement in IVRt (remained prolonged) despite the increase in SR  $\text{Ca}^{2+}$ -uptake. The elevation in  $\text{Ca}^{2+}$ -uptake in PO rats could be correlated with the increase in the level of SERCA2a and increased PLB phosphorylation at both Ser16 and Thr17 residues. As previous studies have shown, there is a direct link between cardiac contractility and the level of expression of key SR-associated  $\text{Ca}^{2+}$ -handling proteins (184,246,247). In particular, SERCA2a is a major player in cardiac contractile performance, as demonstrated by Schultz et al. (248). Their study assessed the role of chronically reduced SERCA2a levels in PO mice and demonstrated that after 10 weeks of aortic banding no mice went into failure, while almost two-thirds of mice heterozygous for SERCA2a went into heart failure stages. Therefore retaining SERCA2a function is critical in maintaining adequate cardiac performance. Arai et al. (243) have shown that the downregulation of SERCA2a gene reduced  $\text{Ca}^{2+}$ -uptake and led to severe hypertrophy in the instances of PO. Gupta et al. (203) showed that PO in rats via the 1K1C procedure reduced SERCA2a expression, which led to decreased  $\text{Ca}^{2+}$ -uptake after 8 weeks, and resulted in pulmonary congestion and heart failure (decompensation).

The chronic effects of PO on cardiac function and concurrent status of the SR in rats have been examined by others (230,249). Ohkusa et al. (230) have shown elevated

SR  $\text{Ca}^{2+}$ -uptake at an early compensated stage of hypertrophy (4 weeks), a time point which was associated with improved cardiac function (systolic and diastolic function) in male Wistar rats. At a later stage, 8 weeks, Ohkusa et al. (230) still showed improved cardiac function despite normalized SR activity. We also show an improvement in SR  $\text{Ca}^{2+}$ -uptake at 4 weeks which, however, was not correlated with an improvement in cardiac function – systolic function was normal and diastolic function was impaired in our study at this time point. Important to note is that the discrepancies between the study by Ohkusa et al. (230) and our work could be due to the differences between rat species and the methods used to assess cardiac function. In another study, Qi et al. (249) examined cardiac and SR function in aortic banded male rats at 8 and 16 weeks. In agreement with our study, Qi et al. (249) also reported diastolic impairment in their 16-week PO rats as well as at earlier time points. However, while a significant reduction in SR activity was observed by Qi et al. (249), this being attributed to reduced levels of SERCA2a, our 16-week PO rats showed the enhancement in SR  $\text{Ca}^{2+}$ -uptake and elevated levels of SERCA2a despite impaired myocardial relaxation. Similarities between this study and our work relate primarily to the fact that progressive deterioration of cardiac function between 8 and 16 weeks, as observed by Qi et al. (249), and between 16 and 28 weeks, as observed by us, is paralleled by a decline in the SR activity/SERCA2a levels or the normalization, respectively.

Few studies have examined the effect of chronic VO on cardiac function, SR  $\text{Ca}^{2+}$ -uptake and phosphorylation of PLB. Hisamatsu et al. (163) observed reduced SR  $\text{Ca}^{2+}$ -uptake without any impairment in cardiac function in 12-week VO rats. Nediani et al. (250) showed a slight reduction in SR  $\text{Ca}^{2+}$ -uptake in 4-week VO pigs, but there were

no alterations at the 8 or 12-week stage of VO; SERCA2a levels were downregulated at all time points while PLB levels or its phosphorylation status (Ser16- PLB) were unaltered at all time points (4, 8 and 12 weeks); cardiac function was only altered at the 4-week stage of volume overload. These results are at variance with our study which showed no alterations in SR  $\text{Ca}^{2+}$ -uptake or cardiac function at the 2- and 4-week stages of VO but increased SR  $\text{Ca}^{2+}$ -uptake and significant alterations in cardiac function after 16 weeks of VO. The difference between the results of these studies and our study could be attributed to the species specific response, to the stimuli, the age of the animals at the time of induction of VO, the size of the AV shunt or the methods used to measure heart function.

It is unknown, however, to what extent the phosphorylation of PLB versus the overexpression of SERCA2a contributed to the increased  $\text{Ca}^{2+}$ -uptake in PO at 16 weeks. In our study, the only significant change observed was in the level of SERCA2a at 16 weeks. With regard to total PLB (both phosphorylated and unphosphorylated), hypertrophic stimuli had no effect on its level of expression within the SR membrane. This finding is highly significant, as the PLB:SERCA2a ratio is a useful determinant of the ability of the SR to take up  $\text{Ca}^{2+}$ . Without a corresponding increase in PLB levels at 16 weeks, the disproportionately higher levels of SERCA2a as detected in both PO and VO at this stage may be free from inhibition and thus able to take up  $\text{Ca}^{2+}$  at a greater rate as was observed.

At 28 weeks,  $\text{Ca}^{2+}$ -uptake returned to sham control levels in the banded (PO) group, but remained significantly elevated in AV shunted (VO) rats. The elevation in SR  $\text{Ca}^{2+}$ -uptake in 28-week VO rats, however, was not as much as seen at the 16-week time

point, however, the diastolic function remained improved (decreased IVRt) similar to that observed at the 16-week time point. Increased SR  $\text{Ca}^{2+}$ -uptake did not correspond to a proportional increase in SERCA2a protein level in 28-week VO hearts. On the contrary, SERCA2a levels were normalized (to sham control levels). Furthermore, phosphorylation of PLB at Ser16 and Thr17 was severely downregulated and this decrease was associated with reduced activities of SR-associated PKA and CaMKII, respectively, and increased SR-associated phosphatase activity. Despite normalized SERCA2a protein levels and severe inhibition of SERCA2a by dephosphorylated PLB at the 28-week time point,  $\text{Ca}^{2+}$ -uptake was still enhanced; it therefore appears that other compensatory mechanisms may be involved in maintaining the hyperfunctional state of SERCA2a in VO. One such mechanism could be an increase in the activity of acylphosphatase, a cytosolic enzyme that hydrolyzes acyl-phosphorylated (EP) intermediate of SERCA thus enhancing the activity of the SERCA pump (251). It is, however, tempting to speculate that any further reduction in PLB phosphorylation could compromise SR  $\text{Ca}^{2+}$ -uptake and diastolic function, thereby triggering the transition from the early stage to the overt stage of heart failure.

Unlike improved diastolic function observed in 28-week VO hearts, PO rats continued to show diastolic dysfunction. Regarding the protein levels, in contrast to 28-week VO group, the decline in SERCA2a protein content back to control levels as well as concurrent reduction in phosphorylation of PLB may be sufficient to explain the normalization in SR  $\text{Ca}^{2+}$ -uptake in 28-week PO rats. The reduction in PLB phosphorylation status is known to occur in diseased heart and it has been documented that in post MI induced heart failure the levels of Ser16-PLB were reduced while those of

Thr17-PLB were unchanged (252). Again, between the changes in PLB phosphorylation and SERCA2a levels the extent to which either contributes to overall  $\text{Ca}^{2+}$ -uptake by the SR is unknown. The examination of PKA and CaMKII activity in PO at the 28-week time point revealed no change in PKA, while CaMKII was slightly but significantly elevated. The reduction in the phosphorylation of PLB at Ser16 and Thr17 signifies that PKA and CaMKII served other cellular purposes, or were cancelled out by concurrently elevated phosphatase activity. In PO, the elevation in phosphatase activity was comparable to VO and was alone enough to cause and perhaps explain the marked dephosphorylation of PLB despite the slight increase in CaMKII activity. Increased CaMKII activity is a condition commonly found in disease states and possibly reflects  $\text{Ca}^{2+}$  handling impairments and  $\text{Ca}^{2+}$  overload which might lead to enhancement in CaMKII activity in the instances of PO. The elevation of CaMKII activity has been shown to occur in failing rabbit hearts (253) and human hearts (254). Similar to our PO results, Huang et al. (255) demonstrated the reduction in both Ser16-PLB and Thr17-PLB phosphorylation that was associated with the elevation of phosphatase activity in post-MI prior to the onset of overt heart failure in rats exhibiting diastolic impairment. Sande et al. (252) showed an association between reduced Ser16-PLB phosphorylation and upregulation of phosphatases (PP1 and PP2A), which depressed SERCA2a activity, and SR  $\text{Ca}^{2+}$ -uptake in rats which were in an overt stage of heart failure. In addition, CaMKII can also act as a direct modulator of SERCA2a as it has been shown that it can directly phosphorylate and therefore stimulate  $\text{Ca}^{2+}$  re-uptake by the SR (130-132). Although, highly speculative at this point the increase in CaMKII activity in PO rats might thus be an adaptive response aimed at minimizing further deterioration of myocardial relaxation by preserving  $\text{Ca}^{2+}$ -

uptake via enhancement of SERCA2a activity in the face of decreased PLB phosphorylation.

### Summary

The findings obtained from echocardiographic assessment of LV geometry demonstrate characteristics of concentric remodelling in PO animals, whereas VO resulted in eccentric remodeling of the LV chamber. Differences between PO and VO rats were also observed when cardiac function was examined. Systolic dysfunction was evident in 28-week PO, while in the case of VO, the dysfunction was apparent at 16 and 28 weeks. Diastolic function was impaired in 4, 16, and 28-week PO rats, while VO rats exhibited an enhanced diastolic function at all time points. SR alterations in the PO model seem to progress faster than in VO. SR  $\text{Ca}^{2+}$ -uptake becomes elevated earlier in PO than in VO, and it also normalizes at the end point (28 weeks) while in VO the activity of the SR still remains high. The normalization in SR  $\text{Ca}^{2+}$ -uptake in 28-week PO rats may be a contributor to the systolic dysfunction observed at this time point. It is unclear whether in VO the improved diastolic function is associated with augmented SR  $\text{Ca}^{2+}$ -uptake at 16 and 28 weeks.

In PO, the increased  $\text{Ca}^{2+}$ -uptake at 16 weeks was associated with increased levels of SERCA2a and increased phosphorylation of PLB at Ser16 and Thr17 residues. At 28 weeks, the normalization of SR  $\text{Ca}^{2+}$ -uptake was due to a normalization of SERCA2a levels, dephosphorylation of PLB at Ser16 and Thr17, and increased protein phosphatase activity. The increased  $\text{Ca}^{2+}$ -uptake in 16-week VO rats was most likely due to increased levels of SERCA2a protein, while at 28 weeks no such association was observed (SR  $\text{Ca}^{2+}$ -uptake was elevated while SERCA2a was normalized and PLB was

dephosphorylated). It is clear, however, that the reduction in PLB phosphorylation was associated with elevated PP activity in both 28-week PO and VO.

The decrease or normalization in SR-associated SERCA2a protein expression in our model of PO is likely the major contributing factor to leveling off of SR  $\text{Ca}^{2+}$ -uptake and possibly systolic dysfunction (at the 28-week time point). Although at later stages (28 weeks) VO rats exhibited the same pattern of SERCA2a and PLB phosphorylation status and expression as PO rats, the enhanced SR  $\text{Ca}^{2+}$ -uptake and improved diastolic function in VO rats was unexpected in this setting of normalized SERCA2a levels, decreased levels of phosphorylated form PLB, decreased kinase (PKA and CaMKII) and increased protein phosphatase activities. Based on what we observed, this mechanism of promoting diastolic  $\text{Ca}^{2+}$ -uptake, in the instances of VO, could be independent of the level/status of SERCA2a and PLB.

### **Conclusions & Future Directions**

One can speculate that PO- and VO-induced hypertrophies share some common pathways leading to some similarities in the way the function of the SR is regulated. At the same time, however, some of the responses evoked by VO are distinct from those generated by PO as this and previous studies have shown (199,227-229). It is possible then that PO and VO rely on different stretch receptors leading to the differences in the phenotype as well as in the recruitment of underlying molecular pathways.

Clearly, there might be other important mediators of  $\text{Ca}^{2+}$  movements across the SR membrane besides the ones examined in this work. In that regard, one of our next goals would be to examine SR  $\text{Ca}^{2+}$ -release which is one of the major determinants of cardiac systolic function. The investigation of SR  $\text{Ca}^{2+}$ -release, as well as the levels and



the status of key SR proteins involved in this process, such as RyR2 and FKBP12.6, will be useful in obtaining a more complete picture of SR  $\text{Ca}^{2+}$  handling processes and their relation to cardiac function in the settings of PO and VO. Identifying the exact mechanism that maintains SR function in VO would also be useful, as the discovery of such could also be applied in the treatment of PO-induced hypertrophy which is a far more prevalent condition in a clinical setting of heart failure.

The question we want to answer in the future is: what allows the SR in VO heart to be “immune” to increased phosphatase activity? It would also be interesting to target phosphatases in an attempt to restore SR function in our model of PO. It has been shown that inhibition of type I phosphatase (PPI) prevents the progression of heart failure (119,193). Besides affecting the phosphorylation status and activity of RyR2, SERCA2a, and PLB, increased phosphatase activity would also have an effect on many other target molecules, including genes. It has been shown that the calcineurin (type 2B phosphatase)/NFAT pathway becomes activated in instances of hemodynamic stress, such as PO, leading to the expression of fetal genes and playing an important role in pathological cardiac hypertrophy and heart failure (119,256-258). It would thus be interesting to determine which phosphatases have a dominant role in our models and whether their inhibition would benefit the overloaded heart.

No study has mapped the profile of cardiac proteins during the development and progression of cardiac hypertrophy induced by PO or VO. Exploring the whole protein profile of the SR, therefore, might lead to a discovery of other important, but, as of yet, unknown or un(der)appreciated molecular mediators of hypertrophy in both PO and VO. Upon identification of potential target proteins, gene manipulation strategies could be

used to overexpress or knockout these proteins in hearts of normal mice. Subjecting these mice to VO or PO could, in turn, reveal whether these genetically modified animals would be resistant to the development of cardiac hypertrophy.

## VII. REFERENCES

1. Opie LH. Heart Physiology – From Cell to Circulation, 4<sup>th</sup> Edition. Lipincott Williams & Wilkins, Philadelphia, PA, 2004.
2. Shariff S, Straatman L, Allard M, Ignaszewski A. Novel associations of giant cell myocarditis: two case reports and a review of the literature. *Can J Cardiol* 2004; 20: 557-61.
3. Scognamiglio R, Avoraro A, Negut C, Piccolotto R, Vigili de Kreutzenberg S, Tiengo A. Early myocardial dysfunction in the diabetic heart: current research and clinical applications. *Am J Cardiol* 2004; 93: 17A-20A.
4. Hilfiker-Kleiner D, Landmesser U, Drexler H. Molecular mechanisms in heart failure focus on cardiac hypertrophy, inflammation, angiogenesis, and apoptosis. *J Am Coll Cardiol* 2006;48(9 Suppl):A56-66.
5. Bukharovich IF, Kukin M; "Cardiac Resynchronization Therapy," Progress in Cardiovascular Disease. Optimal medical therapy for heart failure. *Prog Cardiovasc Dis.* 2006;48:372-85.
6. Hwang JJ, Dzau VJ, Liew CC. Genomics and the pathophysiology of heart failure. *Curr Cardiol Rep.* 2001;3:198-207.
7. Gradman AH, Alfayoumi F. From left ventricular hypertrophy to congestive heart failure: management of hypertensive heart disease. *Prog Cardiovasc Dis.* 2006;48:326-41.
8. Tamargo J, Lopez-Sendon J. Rationale and clinical evidence for the effects of new pharmacological treatments for heart failure. *Rev Esp Cardiol* 2004; 57: 447-64.

9. Kaye DM, Krum H. Drug discovery for heart failure: a new era or the end of the pipeline? *Nat Rev Drug Discov* 2007;6:127-39.
10. Lips DJ, deWindt LJ, van Kraaij DJ, Doevendans PA. Molecular determinants of myocardial hypertrophy and failure: alternative pathways for beneficial and maladaptive hypertrophy. *Eur Heart J* 2003;24:883-96.
11. Prasad K, Kalra J. Oxygen free radicals and heart failure. *Angiology* 1988;39:417-20. Erratum in: *Angiology* 1988 Oct;39(10):927.
12. Landmesser U, Drexler H. Chronic heart failure: an overview of conventional treatment versus novel approaches. *Nat Clin Pract Cardiovasc Med* 2005;2:628-38.
13. Braunwald E, Bristow MR. Congestive heart failure: fifty years of progress. *Circulation* 2000;102(20 Suppl 4):IV14-23.
14. Kerkela R, Force T. Recent insights into cardiac hypertrophy and left ventricular remodeling. *Curr Heart Fail Rep* 2006;3:14-8.
15. Fiorillo C, Nediani C, Ponziani V, Giannini L, Celli A, Nassi N, Formigli L, Perna AM, Nassi P. Cardiac volume overload rapidly induces oxidative stress-mediated myocyte apoptosis and hypertrophy. *Biochim Biophys Acta* 2005;1741:173-82.
16. Opie LH, Commerford PJ, Gersh BJ, Pfeffer MA. Controversies in ventricular remodelling. *Lancet* 2006;367:356-67.
17. Singh N, Dhalla AK, Seneviratne C, Singal PK. Oxidative stress and heart failure. *Mol Cell Biochem.* 1995;147:77-81.
18. Dhalla AK, Hill MF, Singal PK. Role of oxidative stress in transition of hypertrophy to heart failure. *J Am Coll Cardiol.* 1996;28:506-14.

19. Li JM, Gall NP, Grieve DJ, Chen M, Shah AM. Activation of NADPH oxidase during progression of cardiac hypertrophy to failure. *Hypertension* 2002;40:477-84.
20. Arouma OI. Nutrition and health aspects of free radicals and antioxidants. *Food Chem Toxicol* 1994;32:671-83. Erratum in: *Food Chem Toxicol* 1994;32:1185.
21. Calabrese V, Guagliano E, Sapienza M, Mancuso C, Butterfield DA, Stella AM. Redox regulation of cellular stress response in neurodegenerative disorders. *Ital J Biochem* 2006;55:263-82.
22. Cantor EJ, Mancini EV, Seth R, Yao XH, Netticadan T. Oxidative stress and heart disease: cardiac dysfunction, nutrition, and gene therapy. *Curr Hypertens Rep* 2003;5:215-20.
23. Kuster GM, Kotlyar E, Rude MK, Siwik DA, Liao R, Colucci WS, Sam F. Mineralocorticoid receptor inhibition ameliorates the transition to myocardial failure and decreases oxidative stress and inflammation in mice with chronic pressure overload. *Circulation* 2005;111:420-7.
24. Stas S, Whaley-Connell A, Habibi J, Appesh L, Hayden MR, Karuparthi PR, Qazi M, Morris EM, Cooper SA, Link CD, Stump C, Hay M, Ferrario C, Sowers JR. Mineralocorticoid Receptor Blockade Attenuates Chronic Overexpression of the Renin-Angiotensin-Aldosterone System Stimulation of NADPH Oxidase and Cardiac Remodeling. *Endocrinology* 2007; [Epub ahead of print]
25. Landmesser U, Spiekermann S, Dikalov S, Tatge H, Wilke R, Kohler C, Harrison DG, Hornig B, Drexler H. Vascular oxidative stress and endothelial dysfunction in patients with chronic heart failure: role of xanthine-oxidase and extracellular superoxide dismutase. *Circulation* 2002;106:3073-8.

26. Jones SP, Greer JJ, van Haperen R, Duncker DJ, de Crom R, Lefer DJ. Endothelial nitric oxide synthase overexpression attenuates congestive heart failure in mice. *Proc Natl Acad Sci U S A* 2003;100:4891-6.
27. Casademont J, Miro O. Electron transport chain defects in heart failure. *Heart Fail Rev* 2002;7:131-9.
28. Sheeran FL, Pepe S. Energy deficiency in the failing heart: linking increased reactive oxygen species and disruption of oxidative phosphorylation rate. *Biochim Biophys Acta* 2006;1757:543-52.
29. Ferrari R, Guardigli G, Mele D, Percoco GF, Ceconi C, Curello S. Oxidative stress during myocardial ischaemia and heart failure. *Curr Pharm Des* 2004;10:1699-711.
30. De Boer RA, Pinto YM, Van Veldhuisen DJ. The imbalance between oxygen demand and supply as a potential mechanism in the pathophysiology of heart failure: the role of microvascular growth and abnormalities. *Microcirculation* 2003;10:113-26.
31. Katz AM. *Physiology of the Heart*, 3<sup>rd</sup> Edition. Lippincott Williams & Wilkins, Philadelphia, PA, 2001.
32. van Empel VP, Bertrand AT, Hofstra L, Crijns HJ, Doevendans PA, De Windt LJ. Myocyte apoptosis in heart failure. *Cardiovasc Res* 2005;67:21-9.
33. Foo RS, Mani K, Kitsis RN. Death begets failure in the heart. *J Clin Invest* 2005;115:565-71.
34. Wencker D, Chandra M, Nguyen K, Miao W, Garantziotis S, Factor SM, Shirani J, Armstrong RC, Kitsis RN. A mechanistic role for cardiac myocyte apoptosis in heart failure. *J Clin Invest* 2003;111:1497-504.

35. Hayakawa Y, Chandra M, Miao W, Shirani J, Brown JH, Dorn GW 2nd, Armstrong RC, Kitsis RN. Inhibition of cardiac myocyte apoptosis improves cardiac function and abolishes mortality in the peripartum cardiomyopathy of Galpha(q) transgenic mice. *Circulation* 2003;108:3036-41.
36. Chandrashekhar Y, Sen S, Anway R, Shuros A, Anand I. Long-term caspase inhibition ameliorates apoptosis, reduces myocardial troponin-I cleavage, protects left ventricular function, and attenuates remodeling in rats with myocardial infarction. *J Am Coll Cardiol* 2004;43:295-301.
37. Frey N, Olson EN. Cardiac hypertrophy: the good, the bad, and the ugly. *Annu Rev Physiol* 2003;65:45-79.
38. Spinale FG, Coker ML, Heung LJ, Bond BR, Gunasinghe HR, Etoh T, Goldberg AT, Zellner JL, Crumbley AJ. A matrix metalloproteinase induction/activation system exists in the human left ventricular myocardium and is upregulated in heart failure. *Circulation* 2000;102:1944-9.
39. Bristow MR, Ginsburg R, Minobe W, Cubicciotti RS, Sageman WS, Lurie K, Billingham ME, Harrison DC, Stinson EB. Decreased catecholamine sensitivity and beta-adrenergic-receptor density in failing human hearts. *N Engl J Med* 1982;307:205-11.
40. Patel MB, Stewart JM, Loud AV, Anversa P, Wang J, Fiegel L, Hintze TH. Altered function and structure of the heart in dogs with chronic elevation in plasma norepinephrine. *Circulation* 1991;84:2091-100.

41. Fan TH, Liang CS, Kawashima S, Banerjee SP. Alterations in cardiac beta-adrenoceptor responsiveness and adenylate cyclase system by congestive heart failure in dogs. *Eur J Pharmacol* 1987;140:123-32.
42. Banfi C, Cavalca V, Veglia F, Brioschi M, Barcella S, Mussoni L, Boccotti L, Tremoli E, Biglioli P, Agostoni P. Neurohormonal activation is associated with increased levels of plasma matrix metalloproteinase-2 in human heart failure. *Eur Heart J* 2005;26:481-8.
43. Mann DL. Inflammatory mediators and the failing heart: past, present, and the foreseeable future. *Circ Res* 2002;91:988-98.
44. Kurdi M, Randon J, Cerutti C, Bricca G. Increased expression of IL-6 and LIF in the hypertrophied left ventricle of TGR(mRen2)27 and SHR rats. *Mol Cell Biochem* 2005;269:95-101.
45. Wollert KC, Taga T, Saito M, Narazaki M, Kishimoto T, Glembotski CC, Vernallis AB, Heath JK, Pennica D, Wood WI, Chien KR. Cardiotrophin-1 activates a distinct form of cardiac muscle cell hypertrophy. Assembly of sarcomeric units in series VIA gp130/leukemia inhibitory factor receptor-dependent pathways. *J Biol Chem* 1996;271:9535-45.
46. Barlucchi L, Leri A, Dostal DE, Fiordaliso F, Tada H, Hintze TH, Kajstura J, Nadal-Ginard B, Anversa P. Canine ventricular myocytes possess a renin-angiotensin system that is upregulated with heart failure. *Circ Res* 2001;88:298-304.
47. Norton GR, Woodiwiss AJ, Gaasch WH, Mela T, Chung ES, Aurigemma GP, Meyer TE. Heart failure in pressure overload hypertrophy. The relative roles of ventricular remodeling and myocardial dysfunction. *J Am Coll Cardiol*. 2002;39:664-71.



48. Klein L, O'Connor CM, Gattis WA, Zampino M, de Luca L, Vitarelli A, Fedele F, Gheorghiade M. Pharmacologic therapy for patients with chronic heart failure and reduced systolic function: review of trials and practical considerations. *Am J Cardiol* 2003;91:18F-40F. Erratum in: *Am J Cardiol* 2003;92:1378.
49. Berenji K, Drazner MH, Rothermel BA, Hill JA. Does load-induced ventricular hypertrophy progress to systolic heart failure? *Am J Physiol Heart Circ Physiol* 2005;289:H8-H16.
50. Melo LG, Pachori AS, Kong D, Gneccchi M, Wang K, Pratt RE, Dzau VJ. Gene and cell-based therapies for heart disease. *FASEB J* 2004;18:648-63.
51. Krum H, Liew D. New and emerging drug therapies for the management of acute heart failure. *Intern Med J* 2003;33:515-20.
52. Sekiguchi K, Li X, Coker M, Flesch M, Barger PM, Sivasubramanian N, Mann DL. Cross-regulation between the renin-angiotensin system and inflammatory mediators in cardiac hypertrophy and failure. *Cardiovasc Res* 2004;63:433-42.
53. Barki-Harrington L, Perrino C, Rockman HA. Network integration of the adrenergic system in cardiac hypertrophy. *Cardiovasc Res* 2004;63:391-402.
54. Bers DM. Cardiac excitation-contraction coupling. *Nature* 2002;415:198-205.
55. Frey N, Katus HA, Olson EN, Hill JA. Hypertrophy of the heart: a new therapeutic target? *Circulation* 2004;109:1580-89.
56. Carabello BA. Concentric versus eccentric remodeling. *J Card Fail* 2002;8:S258-63.
57. Selvetella G, Hirsch E, Notte A, Tarone G, Lembo G. Adaptive and maladaptive hypertrophic pathways: points of convergence and divergence. *Cardiovasc Res* 2004;63:373-80.

58. Carabello BA. Ten frequently asked questions about cardiac hypertrophy. *Cardiol Rev* 2003;11:249-51.
59. Lorell BH, Carabello BA. Left ventricular hypertrophy: pathogenesis, detection, and prognosis. *Circulation* 2000;102:470-9.
60. Rossi MA, Carillo SV. Cardiac hypertrophy due to pressure and volume overload: distinctly different biological phenomena? *Int J Cardiol* 1991;31:133-41.
61. Chambers J. The left ventricle in aortic stenosis: evidence for the use of ACE inhibitors. *Heart* 2006;92(3):420-23.
62. Poliac LC, Barron ME, Maron BJ. Hypertrophic cardiomyopathy. *Anesthesiology* 2006;104:183-92.
63. Chirillo F, Salvador L, Cavallini C. Medical and surgical treatment of chronic mitral regurgitation. *J Cardiovasc Med (Hagerstown)* 2006;7:96-107.
64. Budts W, Gewillig M, Van de Werf F. Left-to-right shunting in common congenital heart defects: which patients are eligible for percutaneous interventions? *Acta Cardiol* 2003;58:199-205.
65. Metivier F, Marchais SJ, Guerin AP, Pannier B, London GM. Pathophysiology of anaemia: focus on the heart and blood vessels. *Nephrol Dial Transplant* 2000; 15 Suppl 3:14-18.
66. Ross, RS. Molecular and mechanical synergy: cross-talk between integrins and growth factor receptors. *Cardiovasc Res* 2004;63:381-90.
67. Lammerding J, Kamm RD, Lee RT. Mechanotransduction in cardiac myocytes. *Ann N Y Acad Sci* 2004;1015:53-70.

68. Brancaccio M, Hirsch E, Notte A, Selvetella G, Lembo G, Tarone G. Integrin signalling: the tug-of-war in heart hypertrophy. *Cardiovasc Res* 2006;70:422-33.
69. Kudoh S, Akazawa H, Takano H, Zou Y, Toko H, Nagai T, Komuro I. Stretch-modulation of second messengers: effects on cardiomyocyte ion transport. *Prog Biophys Mol Biol* 2003;82:57-66.
70. Ahmad F, Seidman JG, Seidman CE. The genetic basis for cardiac remodeling. *Annu Rev Genomics Hum Genet* 2005;6:185-216.
71. Offermanns S. G-proteins as transducers in transmembrane signalling. *Prog Biophys Mol Biol* 2003;83:101-30.
72. Xiao RP. Beta-adrenergic signaling in the heart: dual coupling of the beta2-adrenergic receptor to G(s) and G(i) proteins. *Sci STKE* 2001;2001:RE15.
73. Engelhardt S, Hein L, Wiesmann F and Lohse M.J. Progressive hypertrophy and heart failure in beta1-adrenergic receptor transgenic mice. *Proc Natl Acad Sci U S A* 1999;96:7059-64.
74. Iwase M, Bishop SP, Uechi M, Vatner DE, Shannon RP, Kudej RK, Wight DC, Wagner TE, Ishikawa Y, Homcy CJ, Vatner SF. Adverse effects of chronic endogenous sympathetic drive induced by cardiac Gs alpha overexpression. *Circ Res* 1996;78:517-24.
75. Antos CL, Frey N, Marx SO, Reiken S, Gaburjakova M, Richardson JA, Marks AR, Olson EN. Dilated cardiomyopathy and sudden death resulting from constitutive activation of protein kinase a. *Circ Res* 2001;89:997-1004.

76. Di Fusco F, Hashim S, Anand-Srivastava MB. Volume overload cardiac hypertrophy exhibits decreased expression of g(s)alpha and not of g(i)alpha in heart. *Am J Physiol Cell Physiol* 2000;279:C990-8.
77. Mazzolai L, Nussberger J, Aubert JF, Brunner DB, Gabbiani G, Brunner HR, Pedrazzini T. Blood pressure-independent cardiac hypertrophy induced by locally activated renin-angiotensin system. *Hypertension* 1998;31:1324-30.
78. Higaki J, Aoki M, Morishita R, Kida I, Taniyama Y, Tomita N, Yamamoto K, Moriguchi A, Kaneda Y, Ogihara T. In vivo evidence of the importance of cardiac angiotensin-converting enzyme in the pathogenesis of cardiac hypertrophy. *Arterioscler Thromb Vasc Biol* 2000;20:428-34.
79. Paradis P, Dali-Youcef N, Paradis FW, Thibault G, Nemer M. Overexpression of angiotensin II type I receptor in cardiomyocytes induces cardiac hypertrophy and remodeling. *Proc Natl Acad Sci U S A* 2000;97(2):931-36.
80. Yang LL, Gros R, Kabir MG, Sadi A, Gotlieb AI, Husain M, Stewart DJ. Conditional cardiac overexpression of endothelin-1 induces inflammation and dilated cardiomyopathy in mice. *Circulation* 2004;109:255-61.
81. Takeishi Y, Ping P, Bolli R, Kirkpatrick DL, Hoit BD, Walsh RA. Transgenic overexpression of constitutively active protein kinase C epsilon causes concentric cardiac hypertrophy. *Circ Res* 2000;86:1218-23.
82. Bowman JC, Steinberg SF, Jiang T, Geenen DL, Fishman GI, Buttrick PM. Expression of protein kinase C $\beta$  in the heart causes hypertrophy in adult mice and sudden death in neonates. *J Clin Invest* 1997;100:2189-95.

83. Nishikawa K, Yoshida M, Kusuhashi M, Ishigami N, Isoda K, Miyazaki K, Ohsuzu F. Left ventricular hypertrophy in mice with a cardiac-specific overexpression of interleukin-1. *Am J Physiol Heart Circ Physiol* 2006;291:H176-H83.
84. Tanaka T, Kanda T, Itoh T, Tsugawa H, Takekoshi N, Yamakawa J, Kurimoto M, Kurabayashi M. Increased cardiac weight in interleukin-6 transgenic mice with viral infection accompanies impaired expression of natriuretic peptide genes. *Res Commun Mol Pathol Pharmacol* 2001;110:275-83.
85. Kubota T, McTiernan CF, Frye CS, Slawson SE, Lemster BH, Koretsky AP, Demetris AJ, Feldman AM. Dilated cardiomyopathy in transgenic mice with cardiac-specific overexpression of tumor necrosis factor- $\alpha$ . *Circ Res* 1997;81:627-35.
86. Sarkar S, Leaman DW, Gupta S, Sil P, Young D, Morehead A, Mukherjee D, Ratliff N, Sun Y, Rayborn M, Hollyfield J, Sen S. Cardiac overexpression of myotrophin triggers myocardial hypertrophy and heart failure in transgenic mice. *J Biol Chem* 2004;279:20422-34.
87. Ponten A, Li X, Thoren P, Aase K, Sjoblom T, Ostman A, Eriksson U. Transgenic overexpression of platelet-derived growth factor-C in the mouse heart induces cardiac fibrosis, hypertrophy, and dilated cardiomyopathy. *Am J Pathol* 2003;163:673-82.
88. Rosenkranz S, Flesch M, Amann K, Haeuseler C, Kilter H, Seeland U, Schluter KD, Bohm M. Alterations of beta-adrenergic signaling and cardiac hypertrophy in transgenic mice overexpressing TGF- $\beta$ (1). *Am J Physiol Heart Circ Physiol* 2002;283:H1253-H62.

89. Hassankhani A, Steinhilper ME, Soonpaa MH, Katz EB, Taylor DA, Andrade-Rozental A, Factor SM, Steinberg JJ, Field LJ, Federoff HJ. Overexpression of NGF within the heart of transgenic mice causes hyperinnervation, cardiac enlargement, and hyperplasia of ectopic cells. *Dev Biol* 1995;169:309-21.
90. Hardt SE, Sadoshima J. Negative regulators of cardiac hypertrophy. *Cardiovasc Res* 2004;63:500-9.
91. Van Empel VP, De Windt LJ. Myocyte hypertrophy and apoptosis: a balancing act. *Cardiovasc Res* 2004;63:487-99.
92. McMullen JR, Izumo S. Role of the insulin-like growth factor 1 (IGF1)/phosphoinositide-3-kinase (PI3K) pathway mediating physiological cardiac hypertrophy. *Novartis Found Symp* 2006;274:90-111.
93. Maron BJ, Pelliccia A. The heart of trained athletes: cardiac remodeling and the risks of sports, including sudden death. *Circulation* 2006;114:1633-44.
94. Mitchell JH, Haskell W, Snell P, Van Camp SP. Task Force 8: classification of sports. *J Am Coll Cardiol* 2005;45:1364-7.
95. Dorn GW 2nd, Force T. Protein kinase cascades in the regulation of cardiac hypertrophy. *J Clin Invest* 2005;115:527-37.
96. McMullen JR, Shioi T, Zhang L, Tarnavski O, Sherwood MC, Kang PM, Izumo S. Phosphoinositide 3-kinase(p110alpha) plays a critical role for the induction of physiological, but not pathological, cardiac hypertrophy. *Proc Natl Acad Sci U S A* 2003;100:12355-60.
97. Heineke J, Molkentin JD. Regulation of cardiac hypertrophy by intracellular signalling pathways. *Nat Rev Mol Cell Biol* 2006;7:589-600.

98. Oudit GY, Sun H, Kerfant BG, Crackower MA, Penninger JM, Backx PH. The role of phosphoinositide-3 kinase and PTEN in cardiovascular physiology and disease. *J Mol Cell Cardiol* 2004;37:449-71.
99. DeBosch B, Treskov I, Lupu TS, Weinheimer C, Kovacs A, Courtois M, Muslin AJ. Akt1 is required for physiological cardiac growth. *Circulation* 2006;113:2097-104.
100. McMullen JR, Amirahmadi F, Woodcock EA, Schinke-Braun M, Bouwman RD, Hewitt KA, Mollica JP, Zhang L, Zhang Y, Shioi T, Buerger A, Izumo S, Jay PY, Jennings GL. Protective effects of exercise and phosphoinositide 3-kinase(p110alpha) signaling in dilated and hypertrophic cardiomyopathy. *Proc Natl Acad Sci U S A* 2007;104:612-7.
101. Barry WH, Bridge JH. Intracellular calcium homeostasis in cardiac myocytes. *Circulation* 1993;87:1806-15.
102. Eisner DA, Choi HS, Diaz ME, O'Neill SC, Trafford AW. Integrative analysis of calcium cycling in cardiac muscle. *Circ Res* 2000;87:1087-94.
103. Katz AM, Lorell BH. Regulation of cardiac contraction and relaxation. *Circulation* 2000;102(20 Suppl 4):IV69-74.
104. Bassani JW, Bassani RA, Bers DM. Relaxation in rabbit and rat cardiac cells: species-dependent differences in cellular mechanisms. *J Physiol* 1994;476:279-93.
105. Bers DM. Ca transport during contraction and relaxation in mammalian ventricular muscle. In: Hasenfuss G, Just H, eds. *Alterations of Excitation-Contraction Coupling in the Failing Human Heart*. New York, NY: Springer-Verlag: 1-16, 1998.
106. MacLennan DH, Kranias EG. Phospholamban: a crucial regulator of cardiac contractility. *Nat Rev Mol Cell Biol* 2003;4:566-77.

107. Frank K, Kranias EG. Phospholamban and cardiac contractility. *Ann Med* 2000;32:572-8.
108. Koss LK, Kranias EG. Phospholamban: A prominent regulator of myocardial contractility. *Circ Res* 1996;79:1059-63.
109. Frank KF, Bolck B, Erdmann E, Schwinger RH. Sarcoplasmic reticulum  $\text{Ca}^{2+}$ -ATPase modulates cardiac contraction and relaxation. *Cardiovasc Res* 2003;57:20-7.
110. Periasamy M, Huke S. SERCA pump level is a critical determinant of  $\text{Ca}^{2+}$  homeostasis and cardiac contractility. *J Mol Cell Cardiol* 2001;33:1053-63.
111. Shannon TR, Ginsburg KS, Bers DM. Reverse mode of the sarcoplasmic reticulum calcium pump and load-dependent cytosolic calcium decline in voltage-clamped cardiac ventricular myocytes. *Biophys J* 2000;78:322-33.
112. Bers DM. Macromolecular complexes regulating cardiac ryanodine receptor function. *J Mol Cell Cardiol* 2004;37:417-29.
113. Lehnart SE, Wehrens XH, Kushnir A, Marks AR. Cardiac ryanodine receptor function and regulation in heart disease. *Ann N Y Acad Sci* 2004;1015:144-59.
114. Beard NA, Casarotto MG, Wei L, Varsanyi M, Laver DR, Dulhunty AF. Regulation of ryanodine receptors by calsequestrin: effect of high luminal  $\text{Ca}^{2+}$  and phosphorylation. *Biophys J* 2005;88:3444-54.
115. Beard NA, Laver DR, Dulhunty AF. Calsequestrin and the calcium release channel of skeletal and cardiac muscle. *Prog Biophys Mol Biol* 2004;85:33-69.
116. MacDougall LK, Jones LR, Cohen P. Identification of the major protein phosphatases in mammalian cardiac muscle which dephosphorylate phospholamban. *Eur J Biochem* 1991;196:725-34.



117. Wehrens XH, Lehnart SE, Reiken S, Vest JA, Wronska A, Marks AR. Ryanodine receptor/calcium release channel PKA phosphorylation: a critical mediator of heart failure progression. *Proc Natl Acad Sci U S A*. 2006;103:511-8.
118. Bers DM. Cardiac ryanodine receptor phosphorylation: target sites and functional consequences. *Biochem J* 2006;396:e1-3.
119. Chakraborti S, Das S, Kar P, Ghosh B, Samanta K, Kolley S, et al. Calcium signaling phenomena in heart diseases: a perspective. *Mol Cell Biochem*. 2007;298:1-40.
120. Colledge M, Scott JD. AKAPs: from structure to function. *Trends Cell Biol* 1999;9:216-21.
121. Rapundalo ST. Cardiac protein phosphorylation: functional and pathophysiological correlates. *Cardiovasc Res* 1998;38:559-88.
122. Kranias EG. Regulation of  $\text{Ca}^{2+}$  transport by cyclic 3',5'-AMP-dependent and calcium-calmodulin-dependent phosphorylation of cardiac sarcoplasmic reticulum. *Biochim Biophys Acta* 1985;844:193-9.
123. Baltas LG, Karczewski P, Bartel S, Krause EG. The endogenous cardiac sarcoplasmic reticulum  $\text{Ca}^{2+}$ /calmodulin-dependent kinase is activated in response to beta-adrenergic stimulation and becomes  $\text{Ca}^{2+}$ -independent in intact beating hearts. *FEBS Lett* 1997;409:131-6.
124. Karczewski P, Kuschel M, Baltas LG, Bartel S, Krause EG. Site-specific phosphorylation of a phospholamban peptide by cyclic nucleotide- and  $\text{Ca}^{2+}$ /calmodulin-dependent protein kinases of cardiac sarcoplasmic reticulum. *Basic Res Cardiol* 1997;92 Suppl 1:37-43.

125. Mattiazzi A, Mundina-Weilenmann C, Guoxiang C, Vittone L, Kranias E. Role of phospholamban phosphorylation on Thr17 in cardiac physiological and pathological conditions. *Cardiovasc Res* 2005;68:366-75.
126. Brittsan AG, Carr AN, Schmidt AG, Kranias EG. Maximal inhibition of SERCA2  $\text{Ca}^{2+}$  affinity by phospholamban in transgenic hearts overexpressing a non-phosphorylatable form of phospholamban. *J Biol Chem* 2000;275:12129-35.
127. Movsesian MA, Colyer J, Wang JH, Krall J. Phospholamban-mediated stimulation of  $\text{Ca}^{2+}$  uptake in sarcoplasmic reticulum from normal and failing hearts. *J Clin Invest* 1990;85:1698-702.
128. Antipenko AY, Spielman AI, Kirchberger MA. Comparison of the effects of phospholamban and jasmone on the calcium pump of cardiac sarcoplasmic reticulum. Evidence for modulation by phospholamban of both  $\text{Ca}^{2+}$  affinity and  $V_{\text{max}}$  (Ca) of calcium transport. *J Biol Chem* 1997;272:2852-60.
129. Kargacin ME, Ali Z, Kargacin G. Anti-phospholamban and protein kinase A alter the  $\text{Ca}^{2+}$  sensitivity and maximum velocity of  $\text{Ca}^{2+}$  uptake by the cardiac sarcoplasmic reticulum. *Biochem J* 1998;331( Pt 1):245-9.
130. Xu A, Hawkins C, Narayanan N. Phosphorylation and activation of the  $\text{Ca}^{2+}$ -pumping ATPase of cardiac sarcoplasmic reticulum by  $\text{Ca}^{2+}$ /calmodulin-dependent protein kinase. *J Biol Chem* 1993;268:8394-7.
131. Hawkins C, Xu A, Narayanan N. Sarcoplasmic reticulum calcium pump in cardiac and slow twitch skeletal muscle but not fast twitch skeletal muscle undergoes phosphorylation by endogenous and exogenous  $\text{Ca}^{2+}$ /calmodulin-dependent protein

- kinase. Characterization of optimal conditions for calcium pump phosphorylation. *J Biol Chem* 1994;269:31198-206.
132. Toyofuku T, Curotto Kurzydowski K, Narayanan N, MacLennan DH. Identification of Ser38 as the site in cardiac sarcoplasmic reticulum  $\text{Ca}^{2+}$ -ATPase that is phosphorylated by  $\text{Ca}^{2+}$ /calmodulin-dependent protein kinase. *J Biol Chem* 1994;269:26492-6.
133. Odermatt A, Kurzydowski K, MacLennan DH. The  $v_{\text{max}}$  of the  $\text{Ca}^{2+}$ -ATPase of cardiac sarcoplasmic reticulum (SERCA2a) is not altered by  $\text{Ca}^{2+}$ /calmodulin-dependent phosphorylation or by interaction with phospholamban. *J Biol Chem* 1996;271:14206-13.
134. Reddy LG, Jones LR, Pace RC, Stokes DL. Purified, reconstituted cardiac  $\text{Ca}^{2+}$ -ATPase is regulated by phospholamban but not by direct phosphorylation with  $\text{Ca}^{2+}$ /calmodulin-dependent protein kinase. *J Biol Chem* 1996;271:14964-70.
135. Takasago T, Imagawa T, Furukawa K, Ogurusu T, Shigekawa M. Regulation of the cardiac ryanodine receptor by protein kinase-dependent phosphorylation. *J Biochem (Tokyo)* 1991;109:163-70.
136. Uehara A, Yasukochi M, Mejia-Alvarez R, Fill M, Imanaga I. Gating kinetics and ligand sensitivity modified by phosphorylation of cardiac ryanodine receptors. *Pflugers Arch* 2002;444:202-12.
137. Valdivia HH, Kaplan JH, Ellis-Davies GC, Lederer WJ. Rapid adaptation of cardiac ryanodine receptors: modulation by  $\text{Mg}^{2+}$  and phosphorylation. *Science* 1995;267:1997-2000.

138. Xiao B, Sutherland C, Walsh MP, Chen SR. Protein kinase A phosphorylation at serine-2808 of the cardiac  $\text{Ca}^{2+}$ -release channel (ryanodine receptor) does not dissociate 12.6-kDa FK506-binding protein (FKBP12.6). *Circ Res* 2004;94:487-95.
139. Wehrens XH, Lehnart SE, Reiken SR, Marks AR.  $\text{Ca}^{2+}$ /calmodulin-dependent protein kinase II phosphorylation regulates the cardiac ryanodine receptor. *Circ Res* 2004;94:e61-70.
140. Rodriguez P, Bhogal MS, Colyer J. Stoichiometric phosphorylation of cardiac ryanodine receptor on serine 2809 by calmodulin-dependent kinase II and protein kinase A. *J Biol Chem* 2003;278:38593-600.
141. Cohen P. The structure and regulation of protein phosphatases. *Annu Rev Biochem* 1989;58:453-508.
142. MacDougall LK, Jones LR, Cohen P. Identification of the major protein phosphatases in mammalian cardiac muscle which dephosphorylate phospholamban. *Eur J Biochem* 1991;196:725-34.
143. Steenaart NA, Ganim JR, Di Salvo J, Kranias EG. The phospholamban phosphatase associated with cardiac sarcoplasmic reticulum is a type 1 enzyme. *Arch Biochem Biophys* 1992;293:17-24.
144. Kranias EG, Di Salvo J. A phospholamban protein phosphatase activity associated with cardiac sarcoplasmic reticulum. *J Biol Chem* 1986;261:10029-32.
145. Bandyopadhyay A, Shin DW, Ahn JO, Kim DH. Calcineurin regulates ryanodine receptor/ $\text{Ca}^{2+}$ -release channels in rat heart. *Biochem J* 2000;352 Pt 1:61-70.
146. Martinez ML, Heredia MP, Delgado C. Expression of T-type  $\text{Ca}^{2+}$  channels in ventricular cells from hypertrophied rat hearts. *J Mol Cell Cardiol* 1999;31:1617-25.

147. Ming Z, Nordin C, Siri F, Aronson RS. Reduced calcium current density in single myocytes isolated from hypertrophied failing guinea pig hearts. *J Mol Cell Cardiol* 1994;26:1133-43.
148. Wang Z, Nolan B, Kutschke W, Hill JA. Na<sup>+</sup>-Ca<sup>2+</sup> exchanger remodeling in pressure overload cardiac hypertrophy. *J Biol Chem* 2001;276:17706-11.
149. Tappia PS, Hata T, Hozaima L, Sandhu MS, Panagia V, Dhalla NS. Role of oxidative stress in catecholamine-induced changes in cardiac sarcolemmal Ca<sup>2+</sup> transport. *Arch Biochem Biophys* 2001;387:85-92.
150. Temsah RM, Netticadan T, Chapman D, Takeda S, Mochizuki S, Dhalla NS. Alterations in sarcoplasmic reticulum function and gene expression in ischemic-reperfused rat heart. *Am J Physiol* 1999;277(2 Pt 2):H584-94.
151. Itoh S, Yanagishita T, Aoki S, Koba S, Iwata T, Ishioka H, Arata H, Mukae S, Geshi E, Konno N, Katagiri T, Utsumi H. Generation of free radicals and the damage done to the sarcoplasmic reticulum during reperfusion injury following brief ischemia in the canine heart. *Jpn Circ J* 1999;63:373-8.
152. Schmidt U, Hajjar RJ, Helm PA, Kim CS, and Gwathmey JK. Contribution of abnormal sarcoplasmic reticulum ATPase activity to systolic and diastolic function in human heart failure. *J Mol Cell Cardiol* 1998;30:1929-37.
153. Yamaguchi F, Sanbe A, and Takeo S. Cardiac sarcoplasmic reticular function in rats with chronic heart failure following myocardial infarction. *J Mol Cell Cardiol* 1997;29:753-63.
154. O'Brien PJ, Moe GW, Nowack LM, Grima EA, and Armstrong PW. Sarcoplasmic reticulum Ca-release channel and ATP synthesis activities are early myocardial

- markers of heart failure produced by rapid pacing in dogs. *Can J Physiol Pharmacol* 1994;72:999-1006.
155. Kiss E, Ball NA, Kranias EG, Walsh RA. Differential changes in cardiac phospholamban and sarcoplasmic reticular  $\text{Ca}^{2+}$ -ATPase protein levels. Effects on  $\text{Ca}^{2+}$  transport and mechanics in compensated pressure-overload hypertrophy and congestive heart failure. *Circ Res* 1995;77:759-64.
156. Rupp H, Vetter R. Sarcoplasmic reticulum function and carnitine palmitoyltransferase-1 inhibition during progression of heart failure. *Br J Pharmacol* 2000;131:1748-56.
157. Matsui H, MacLennan DH, Alpert NR, Periasamy M. Sarcoplasmic reticulum gene expression in pressure overload-induced cardiac hypertrophy in rabbit. *Am J Physiol* 1995;268(1 Pt 1):C252-8.
158. Takeishi Y, Bhagwat A, Ball NA, Kirkpatrick DL, Periasamy M, Walsh RA. Effect of angiotensin-converting enzyme inhibition on protein kinase C and SR proteins in heart failure. *Am J Physiol* 1999;276(1 Pt 2):H53-62.
159. Periasamy M, Reed TD, Liu LH, Ji Y, Loukianov E, Paul RJ, Nieman ML, Riddle T, Duffy JJ, Doetschman T, Lorenz JN, Shull GE. Impaired cardiac performance in heterozygous mice with a null mutation in the sarco(endo)plasmic reticulum  $\text{Ca}^{2+}$ -ATPase isoform 2 (SERCA2) gene. *J Biol Chem* 1999;274:2556-62.
160. Takeshima H, Komazaki S, Hirose K, Nishi M, Noda T, Iino M. Embryonic lethality and abnormal cardiac myocytes in mice lacking ryanodine receptor type 2. *EMBO J* 1998;17:3309-16.

161. Whitmer JT, Kumar P, and Solaro RJ. Calcium transport properties of cardiac sarcoplasmic reticulum from cardiomyopathic Syrian hamsters (BIO 53.58 and 14.6): evidence for a quantitative defect in dilated myopathic hearts not evident in hypertrophic hearts. *Circ Res* 1988;62:81-5.
162. Ueyama T, Ohkusa T, Hisamatsu Y, Nakamura Y, Yamamoto T, Yano M, and Matsuzaki M. Alterations in cardiac SR  $\text{Ca}^{2+}$  release channels during development of heart failure in cardiomyopathic hamsters. *Am J Physiol* 1998;274:H1-H7.
163. Hisamatsu Y, Ohkusa T, Kihara Y, Inoko M, Ueyama T, Yano M, et al. Early changes in the functions of cardiac sarcoplasmic reticulum in volume-overloaded cardiac hypertrophy in rats. *J Mol Cell Cardiol* 1997;29:1097-109.
164. Gibbs CL, Wendt IR, Kotsanas G, Young IR, Woolley G. Mechanical, energetic, and biochemical changes in long-term pressure overload of rabbit heart. *Am J Physiol* 1990;259(3 Pt 2):H849-59.
165. Calderone A, Takahashi N, Izzo NJ Jr, Thaik CM, Colucci WS. Pressure- and volume-induced left ventricular hypertrophies are associated with distinct myocyte phenotypes and differential induction of peptide growth factor mRNAs. *Circulation* 1995;92:2385-90.
166. Boknik P, Heinroth-Hoffmann I, Kirchhefer U, Knapp J, Linck B, Luss H, Muller T, Schmitz W, Brodde O, Neumann J. Enhanced protein phosphorylation in hypertensive hypertrophy. *Cardiovasc Res* 2001;51:717-28.
167. Arata Y, Geshi E, Nomizo A, Aoki S, Katagiri T. Alterations in sarcoplasmic reticulum and angiotensin II receptor type 1 gene expression in spontaneously hypertensive rat hearts. *Jpn Circ J* 1999;63:367-72.

168. Ohta K, Kim S, Hamaguchi A, Miura K, Yukimura T, Iwao H. Expression of sarcoplasmic reticulum  $\text{Ca}^{2+}$ -ATPase mRNA in the hypertrophied heart of young spontaneously hypertensive rats. *Clin Exp Pharmacol Physiol Suppl* 1995;22:S228-9.
169. Shorofsky SR, Aggarwal R, Corretti M, Baffa JM, Strum JM, Al-Seikhan BA, Kobayashi YM, Jones LR, Wier WG, Balke CW. Cellular mechanisms of altered contractility in the hypertrophied heart: big hearts, big sparks. *Circ Res* 1999;84(4):424-34.
170. Neticadan T, Temsah RM, Kawabata K, Dhalla NS. Sarcoplasmic reticulum  $\text{Ca}^{2+}$ /Calmodulin-dependent protein kinase is altered in heart failure. *Circ Res* 2000;86:596-605.
171. Schwinger RH, Munch G, Bolck B, Karczewski P, Krause EG, Erdmann E. Reduced  $\text{Ca}^{2+}$ -sensitivity of SERCA 2a in failing human myocardium due to reduced serin-16 phospholamban phosphorylation. *J Mol Cell Cardiol* 1999;31:479-91.
172. Hagemann D, Bohlender J, Hoch B, Krause EG, Karczewski P. Expression of  $\text{Ca}^{2+}$ /calmodulin-dependent protein kinase II delta-subunit isoforms in rats with hypertensive cardiac hypertrophy. *Mol Cell Biochem* 2001;220:69-76.
173. Pogwizd SM, Qi M, Yuan W, Samarel AM, Bers DM. Upregulation of  $\text{Na}^{+}$ / $\text{Ca}^{2+}$  exchanger expression and function in an arrhythmogenic rabbit model of heart failure. *Circ Res* 1999;85:1009-19.
174. Shannon TR, Pogwizd SM, Bers DM. Elevated sarcoplasmic reticulum  $\text{Ca}^{2+}$  leak in intact ventricular myocytes from rabbits in heart failure. *Circ Res* 2003;93:592-4.



175. Ai X, Curran JW, Shannon TR, Bers DM, Pogwizd SM. Ca<sup>2+</sup>/calmodulin-dependent protein kinase modulates cardiac ryanodine receptor phosphorylation and sarcoplasmic reticulum Ca<sup>2+</sup> leak in heart failure. *Circ Res* 2005;97:1314-22.
176. Marx SO, Reiken S, Hisamatsu Y, Jayaraman T, Burkhoff D, Rosembliit N, Marks AR. PKA phosphorylation dissociates FKBP12.6 from the calcium release channel (ryanodine receptor): defective regulation in failing hearts. *Cell* 2000;101:365-76.
177. Ono K, Yano M, Ohkusa T, Kohno M, Hisaoka T, Tanigawa T, Kobayashi S, Kohno M, Matsuzaki M. Altered interaction of FKBP12.6 with ryanodine receptor as a cause of abnormal Ca(2+) release in heart failure. *Cardiovasc Res* 2000;48:323-31.
178. Milnes JT, MacLeod KT. Reduced ryanodine receptor to dihydropyridine receptor ratio may underlie slowed contraction in a rabbit model of left ventricular cardiac hypertrophy. *J Mol Cell Cardiol* 2001;33:473-85.
179. Kim DH, Mkparu F, Kim CR, Carroll RF. Alteration of Ca<sup>2+</sup> release channel function in sarcoplasmic reticulum of pressure-overload-induced hypertrophic rat heart. *J Mol Cell Cardiol* 1994;26:1505-12.
180. Xu M, Zhou P, Xu SM, Liu Y, Feng X, Bai SH, Bai Y, Hao XM, Han Q, Zhang Y, Wang SQ. Intermolecular failure of L-type Ca<sup>2+</sup> channel and ryanodine receptor signaling in hypertrophy. *PLoS Biol* 2007;5:e21.
181. Raina A, Pickering T, Shimbo D. Statin use in heart failure: a cause for concern? *Am Heart J* 2006;152:39-49.
182. Laufs U, Custodis F, Bohm M. HMG-CoA reductase inhibitors in chronic heart failure: potential mechanisms of benefit and risk. *Drugs* 2006;66:145-54.

183. Takano H, Zou Y, Akazawa H, Toko H, Mizukami M, Hasegawa H, Asakawa M, Nagai T, Komuro I. Inhibitory molecules in signal transduction pathways of cardiac hypertrophy. *Hypertens Res* 2002;25:491-98.
184. Miyamoto MI, del Monte F, Schmidt U, DiSalvo TS, Kang ZB, Matsui T, Guerrero JL, Gwathmey JK, Rosenzweig A, Hajjar RJ. Adenoviral gene transfer of SERCA2a improves left-ventricular function in aortic-banded rats in transition to heart failure. *Proc Natl Acad Sci U S A* 2000;97:793-8.
185. del Monte F, Williams E, Lebeche D, Schmidt U, Rosenzweig A, Gwathmey JK, Lewandowski ED, Hajjar RJ. Improvement in survival and cardiac metabolism after gene transfer of sarcoplasmic reticulum Ca(2+)-ATPase in a rat model of heart failure. *Circulation* 2001;104:1424-9.
186. Hirsch JC, Borton AR, Albayya FP, Russell MW, Ohye RG, Metzger JM. Comparative analysis of parvalbumin and SERCA2a cardiac myocyte gene transfer in a large animal model of diastolic dysfunction. *Am J Physiol Heart Circ Physiol* 2004;286:H2314-21.
187. Hoshijima M, Ikeda Y, Iwanaga Y, Minamisawa S, Date MO, Gu Y, Iwatate M, Li M, Wang L, Wilson JM, Wang Y, Ross J Jr, Chien KR. Chronic suppression of heart-failure progression by a pseudophosphorylated mutant of phospholamban via in vivo cardiac rAAV gene delivery. *Nat Med* 2002;8:864-71.
188. del Monte F, Harding SE, Dec GW, Gwathmey JK, Hajjar RJ. Targeting phospholamban by gene transfer in human heart failure. *Circulation* 2002;105:904-7.
189. Haghighi K, Kolokathis F, Gramolini AO, Waggoner JR, Pater L, Lynch RA, Fan GC, Tsiapras D, Parekh RR, Dorn GW 2nd, MacLennan DH, Kremastinos DT,

- Kranias EG. A mutation in the human phospholamban gene, deleting arginine 14, results in lethal, hereditary cardiomyopathy. *Proc Natl Acad Sci U S A* 2006;103:1388-93.
190. Schmitt JP, Kamisago M, Asahi M, Li GH, Ahmad F, Mende U, Kranias EG, MacLennan DH, Seidman JG, Seidman CE. Dilated cardiomyopathy and heart failure caused by a mutation in phospholamban. *Science* 2003;299:1410-3.
  191. Neumann J, Eschenhagen T, Jones LR, Linck B, Schmitz W, Scholz H, Zimmermann N. Increased expression of cardiac phosphatases in patients with end-stage heart failure. *J Mol Cell Cardiol* 1997;29:265-72.
  192. Gupta RC, Mishra S, Rastogi S, Imai M, Habib O, Sabbah HN. Cardiac SR-coupled PP1 activity and expression are increased and inhibitor 1 protein expression is decreased in failing hearts. *Am J Physiol Heart Circ Physiol* 2003;285:H2373-81.
  193. Pathak A, del Monte F, Zhao W, Schultz JE, Lorenz JN, Bodi I, Weiser D, Hahn H, Carr AN, Syed F, Mavila N, Jha L, Qian J, Marreez Y, Chen G, McGraw DW, Heist EK, Guerrero JL, DePaoli-Roach AA, Hajjar RJ, Kranias EG. Enhancement of cardiac function and suppression of heart failure progression by inhibition of protein phosphatase 1. *Circ Res* 2005;96:756-66.
  194. Marks AR. Novel therapy for heart failure and exercise-induced ventricular tachycardia based on 'fixing' the leak in ryanodine receptors. *Novartis Found Symp* 2006;274:132-47.
  195. Phrommintikul A, Chattipakorn N. Roles of cardiac ryanodine receptor in heart failure and sudden cardiac death. *Int J Cardiol* 2006;112:142-52.

196. Wehrens XH, Lehnart SE, Huang F, Vest JA, Reiken SR, Mohler PJ, Sun J, Guatimosim S, Song LS, Rosembliet N, D'Armiento JM, Napolitano C, Memmi M, Priori SG, Lederer WJ, Marks AR. FKBP12.6 deficiency and defective calcium release channel (ryanodine receptor) function linked to exercise-induced sudden cardiac death. *Cell* 2003;113:829-40.
197. Lehnart SE, Terrenoire C, Reiken S, Wehrens XH, Song LS, Tillman EJ, Mancarella S, Coromilas J, Lederer WJ, Kass RS, Marks AR. Stabilization of cardiac ryanodine receptor prevents intracellular calcium leak and arrhythmias. *Proc Natl Acad Sci U S A* 2006;103:7906-10.
198. Yano M, Kobayashi S, Kohno M, Doi M, Tokuhisa T, Okuda S, Suetsugu M, Hisaoka T, Obayashi M, Ohkusa T, Kohno M, Matsuzaki M. FKBP12.6-mediated stabilization of calcium-release channel (ryanodine receptor) as a novel therapeutic strategy against heart failure. *Circulation* 2003;107:477-84.
199. Cantor EJ, Babick AP, Vasanji Z, Dhalla NS, Netticadan T. A comparative serial echocardiographic analysis of cardiac structure and function in rats subjected to pressure or volume overload. *J Mol Cell Cardiol* 2005;38:777-86.
200. Ganguly PK, Lee SL, Beamish RE, Dhalla NS. Altered sympathetic system and adrenoceptors during the development of cardiac hypertrophy. *Am Heart J* 1989;118:520-5.
201. Hiyoshi H, Yayama K, Takano M, Okamoto H. Stimulation of cyclic GMP production via AT<sub>2</sub> and B<sub>2</sub> receptors in the pressure-overloaded aorta after banding. *Hypertension* 2004;43:1258-63.

202. Liao Y, Ishikura F, Beppu S, Asakura M, Takashima S, Asanuma H, Sanada S, Kim J, Ogita H, Kuzuya T, Node K, Kitakaze M, Hori M. Echocardiographic assessment of LV hypertrophy and function in aortic-banded mice: necropsy validation. *Am J Physiol Heart Circ Physiol* 2002;282:H1703-8.
203. Gupta RC, Yang XP, Mishra S, Sabbah HN. Assessment of sarcoplasmic reticulum  $\text{Ca}^{2+}$ -uptake during the development of left ventricular hypertrophy. *Biochem Pharmacol* 2003;65:933-9.
204. Gupta RC, Mishra S, Yang XP, Sabbah HN. Reduced inhibitor 1 and 2 activity is associated with increased protein phosphatase type 1 activity in left ventricular myocardium of one-kidney, one-clip hypertensive rats. *Mol Cell Biochem* 2005;269:49-57.
205. Lamberts RR, Vaessen RJ, Westerhof N, Stienen GJ. Right ventricular hypertrophy causes impairment of left ventricular diastolic function in the rat. *Basic Res Cardiol*. 2007;102:19-27.
206. Garcia R, Diebold S. Simple, rapid, and effective method of producing aortocaval shunts in the rat. *Cardiovasc Res* 1990;24:430-2.
207. Wang X, Ren B, Liu S, Sentex E, Tappia PS, Dhalla NS. Characterization of cardiac hypertrophy and heart failure due to volume overload in the rat. *J Appl Physiol* 2003;94:752-63.
208. Hashida H, Hamada M, Hiwada K. Serial changes in sarcoplasmic reticulum gene expression in volume-overloaded cardiac hypertrophy in the rat: effect of an angiotensin II receptor antagonist. *Clin Sci (Lond)* 1999;96:387-95.

209. Deroubaix E, Folliguet T, Rucker-Martin C, Dinanian S, Boixel C, Validire P, Daniel P, Capderou A, Hatem SN. Moderate and chronic hemodynamic overload of sheep atria induces reversible cellular electrophysiologic abnormalities and atrial vulnerability. *J Am Coll Cardiol* 2004;44:1918-26.
210. Takahashi N, Atsumi H, Nakada S, Takeishi Y, Tomoike H. Alterations in the inotropic responses to forskolin and  $Ca^{2+}$  and reduced gene expressions of  $Ca^{2+}$ -signaling proteins induced by chronic volume overload in rabbits. *Jpn Circ J* 2000;64:861-7.
211. Tanne Z, Coleman R, Nahir M, Shomrat D, Finberg JP, Youdim MB. Ultrastructural and cytochemical changes in the heart of iron-deficient rats. *Biochem Pharmacol* 1994;47:1759-66.
212. Olivetti G, Quaini F, Lagrasta C, Ricci R, Tiberti G, Capasso JM, Anversa P. Myocyte cellular hypertrophy and hyperplasia contribute to ventricular wall remodeling in anemia-induced cardiac hypertrophy in rats. *Am J Pathol* 1992;141:227-39.
213. Maeba T. Calcium-binding of cardiac sarcoplasmic reticulum and diastolic hemodynamics in volume overloaded canine hearts. *Jpn Circ J* 1985;49:163-70.
214. Matsuo T, Carabello BA, Nagatomo Y, Koide M, Hamawaki M, Zile MR, McDermott PJ. Mechanisms of cardiac hypertrophy in canine volume overload. *Am J Physiol* 1998;275:H65-74.
215. Oyama MA, Sisson DD, Bulmer BJ, Constable PD. Echocardiographic estimation of mean left atrial pressure in a canine model of acute mitral valve insufficiency. *J Vet Intern Med* 2004;18:667-72.

216. Bauman RP, Rembert JC, Greenfield JC Jr. Myocardial blood flow in awake dogs with chronic tricuspid regurgitation. *Basic Res Cardiol* 1998;93:63-9.
217. Murakami K, Mizushige K, Noma T, Kimura S, Abe Y, Matsuo H. Effects of perindopril on left ventricular remodeling and aortic regurgitation in rats assessed by echocardiography. *Angiology* 2000;51:943-52.
218. Sallinen P, Manttari S, Leskinen H, Ilves M, Ruskoaho H, Saarela S. Time course of changes in the expression of DHPR, RyR(2), and SERCA2 after myocardial infarction in the rat left ventricle. *Mol Cell Biochem* 2007; [Epub ahead of print].
219. Sahn DJ, DeMaria A, Kisslo J, Weyman A. Recommendations regarding quantitation in M-mode echocardiography: results of a survey of echocardiographic measurements. *Circulation* 1978;58:1072-83.
220. Vasanji Z, Dhalla NS, Netticadan T. Increased inhibition of SERCA2 by phospholamban in the type I diabetic heart. *Mol Cell Biochem* 2004;261:245-49.
221. Vasanji Z, Cantor EJ, Juric D, Moyan M, Netticadan T. Alterations in cardiac contractile performance and sarcoplasmic reticulum function in sucrose-fed rats is associated with insulin resistance. *Am J Physiol Cell Physiol*. 2006;291:C772-80.
222. Singh RB, Chohan PK, Dhalla NS, Netticadan T. The sarcoplasmic reticulum proteins are targets for calpain action in the ischemic-reperfused heart. *J Mol Cell Cardiol* 2004;37:101-10.
223. Chohan PK, Singh RB, Dhalla NS, Netticadan T. L-arginine administration recovers sarcoplasmic reticulum function in ischemic reperfused hearts by preventing calpain activation. *Cardiovasc Res* 2006;69:153-63.

224. Babick AP, Cantor EJ, Babick JT, Takeda N, Dhalla NS, Netticadan T. Cardiac contractile dysfunction in J2N-k cardiomyopathic hamsters is associated with impaired SR function and regulation. *Am J Physiol Cell Physiol* 2004;287:C1202-8.
225. Lowry OH, Rosebrough NJ, Farr AL, Randall RJ. Protein measurement with the Folin phenol reagent. *J Biol Chem* 1951;193: 265-75.
226. Netticadan T, Temsah RM, Kent A, Elimban V, Dhalla NS. Depressed levels of Ca<sup>2+</sup>-cycling proteins may underlie sarcoplasmic reticulum dysfunction in the diabetic heart. *Diabetes* 2001;50:2133-38.
227. Modesti PA, Vanni S, Bertolozzi I, Cecioni I, Polidori G, Paniccia R, Bandinelli B, Perna A, Liguori P, Boddi M, Galanti G, Sernerri GG. Early sequence of cardiac adaptations and growth factor formation in pressure- and volume-overload hypertrophy. *Am J Physiol Heart Circ Physiol* 2000;279:H976-85.
228. Carabello BA, Zile MR, Tanaka R, Cooper G 4th. Left ventricular hypertrophy due to volume overload versus pressure overload. *Am J Physiol*. 1992;263:H1137-44.
229. Plehn JF, Foster E, Grice WN, Huntington-Coats M, Apstein CS. Echocardiographic assessment of LV mass in rabbits: models of pressure and volume overload hypertrophy. *Am J Physiol* 1993;265:H2066-72.
230. Ohkusa T, Hisamatsu Y, Yano M, Kobayashi S, Tatsuno H, Saiki Y, Kohno M, Matsuzaki M. Altered cardiac mechanism and sarcoplasmic reticulum function in pressure overload-induced cardiac hypertrophy in rats. *J Mol Cell Cardiol* 1997;29:45-54.
231. Carabello BA. Models of volume overload hypertrophy. *J Card Fail* 1996;2:55-64.



232. Zile MR, Tomita M, Nakano K, Mirsky I, Usher B, Lindroth J, Carabello BA. Effects of left ventricular volume overload produced by mitral regurgitation on diastolic function. *Am J Physiol* 1991;261:H1471-80.
233. Salemi VM, Pires MD, Cestari IN, Cestari IA, Picard MH, Leirner AA, Mady C. Echocardiographic assessment of global ventricular function using the myocardial performance index in rats with hypertrophy. *Artif Organs*. 2004;28:332-7.
234. Gutierrez C, Blanchard DG. Diastolic heart failure: challenges of diagnosis and treatment. *Am Fam Physician*. 2004;69:2609-16.
235. Weber KT, Janicki JS, Shroff SG, Pick R, Chen RM, Bashey RI. Collagen remodeling of the pressure-overloaded, hypertrophied nonhuman primate myocardium. *Circ Res* 1988;62:757-65.
236. Jalil JE, Doering CW, Janicki JS, Pick R, Shroff SG, Weber KT. Fibrillar collagen and myocardial stiffness in the intact hypertrophied rat left ventricle. *Circ Res* 1989;64:1041-50.
237. Kuwahara F, Kai H, Tokuda K, Takeya M, Takeshita A, Egashira K, Imaizumi T. Hypertensive myocardial fibrosis and diastolic dysfunction: another model of inflammation? *Hypertension* 2004;43:739-45.
238. Salemi VM, Picard MH, Mady C. Assessment of diastolic function in endomyocardial fibrosis: value of flow propagation velocity. *Artif Organs* 2004;28:343-6.
239. Muller OJ, Lange M, Rattunde H, Lorenzen HP, Muller M, Frey N, Bittner C, Simonides W, Katus HA, Franz WM. Transgenic rat hearts overexpressing

- SERCA2a show improved contractility under baseline conditions and pressure overload. *Cardiovasc Res* 2003;59:380-9.
240. De Stefano LM, Matsubara LS, Matsubara BB. Myocardial dysfunction with increased ventricular compliance in volume overload hypertrophy. *Eur J Heart Fail.* 2006;8:784-9.
241. Dudas Gyorki Z, Kollar A, Manczur F, Kekesi V, Voros K. Echocardiographic characterisation of cardiac dilatation induced by volume overload in a canine experimental model. *Acta Vet Hung* 2007;55:41-50.
242. Boateng S, Seymour AM, Dunn M, Yacoub M, Boheler K. Inhibition of endogenous cardiac phosphatase activity and measurement of sarcoplasmic reticulum calcium uptake: a possible role of phospholamban phosphorylation in the hypertrophied myocardium. *Biochem Biophys Res Commun* 1997;239:701-5.
243. Arai M, Suzuki T, Nagai R. Sarcoplasmic reticulum genes are upregulated in mild cardiac hypertrophy but downregulated in severe cardiac hypertrophy induced by pressure overload. *J Mol Cell Cardiol* 1996;28:1583-90.
244. Carvalho BM, Bassani RA, Franchini KG, Bassani JW. Enhanced calcium mobilization in rat ventricular myocytes during the onset of pressure overload-induced hypertrophy. *Am J Physiol Heart Circ Physiol* 2006;291:H1803-13.
245. Balke CW, Egan TM, Wier WG. Processes that remove calcium from the cytoplasm during excitation-contraction coupling in intact rat heart cells. *J Physiol* 1994;474:447-62.
246. del Monte F, Johnson CM, Stepanek AC, Doye AA, Gwathmey JK. Defects in calcium control. *J Card Fail* 2002;8(6 Suppl):S421-31.

247. del Monte F, Hajjar RJ. Targeting calcium cycling proteins in heart failure through gene transfer. *J Physiol* 2003;546(Pt 1):49-61.
248. Schultz Jel J, Glascock BJ, Witt SA, Nieman ML, Nattamai KJ, Liu LH, Lorenz JN, Shull GE, Kimball TR, Periasamy M. Accelerated onset of heart failure in mice during pressure overload with chronically decreased SERCA2 calcium pump activity. *Am J Physiol Heart Circ Physiol* 2004;286:H1146-53.
249. Qi M, Shannon TR, Euler DE, Bers DM, Samarel AM. Downregulation of sarcoplasmic reticulum Ca(2+)-ATPase during progression of left ventricular hypertrophy. *Am J Physiol* 1997;272(5 Pt 2):H2416-24.
250. Nediani C, Formigli L, Perna AM, Pacini A, Ponziani V, Modesti PA, et al. Biochemical changes and their relationship with morphological and functional findings in pig heart subjected to lasting volume overload: a possible role of acylphosphatase in the regulation of sarcoplasmic reticulum calcium pump. *Basic Res Cardiol* 2002;97:469-78.
251. Nediani C, Celli A, Fiorillo C, Ponziani V, Giannini L, Nassi P. Acylphosphatase interferes with SERCA2a-PLN association. *Biochem Biophys Res Commun* 2003;301:948-51.
252. Sande JB, Sjaastad I, Hoen IB, Bokenes J, Tonnessen T, Holt E, Lunde PK, Christensen G. Reduced level of serine(16) phosphorylated phospholamban in the failing rat myocardium: a major contributor to reduced SERCA2 activity. *Cardiovasc Res* 2002;53:382-91.

253. Currie S, Smith GL. Calcium/calmodulin-dependent protein kinase II activity is increased in sarcoplasmic reticulum from coronary artery ligated rabbit hearts. *FEBS Lett* 1999;459:244-8.
254. Kirchhefer U, Schmitz W, Scholz H, Neumann J. Activity of cAMP-dependent protein kinase and Ca<sup>2+</sup>/calmodulin-dependent protein kinase in failing and nonfailing human hearts. *Cardiovasc Res* 1999;42:254-61.
255. Huang B, Wang S, Qin D, Boutjdir M, El-Sherif N. Diminished basal phosphorylation level of phospholamban in the postinfarction remodeled rat ventricle: role of beta-adrenergic pathway, G(i) protein, phosphodiesterase, and phosphatases. *Circ Res* 1999;85:848-55.
256. Fiedler B, Wollert KC. Targeting calcineurin and associated pathways in cardiac hypertrophy and failure. *Expert Opin Ther Targets* 2005;9:963-73.
257. Diedrichs H, Chi M, Boelck B, Mehlhorn U, Schwinger RH. Increased regulatory activity of the calcineurin/NFAT pathway in human heart failure. *Eur J Heart Fail* 2004 ;6:3-9. Erratum in: *Eur J Heart Fail* 2004;6:823.
258. Wilkins BJ, Dai YS, Bueno OF, Parsons SA, Xu J, Plank DM, Jones F, Kimball TR, Molkentin JD. Calcineurin/NFAT coupling participates in pathological, but not physiological, cardiac hypertrophy. *Circ Res* 2004;94:110-8.